Computational and Structural Biotechnology Journal 23 (2024) 3391–3406

Contents lists available at ScienceDirect

Computational and Structural Biotechnology Journal

journal homepage: www.elsevier.com/locate/csbj

Research Article

Discovery, development and optimisation of a novel frog antimicrobial peptide with combined mode of action against drug-resistant bacteria

Jingkai Wang [a,1], Jibo Hu [a,b,1], Wenyuan Pu [c], Xiaoling Chen [a], Chengbang Ma [a], Yangyang Jiang [a,*], Tao Wang [a,*], Tianbao Chen [a,b], Chris Shaw [a], Mei Zhou [a], Lei Wang [a]

[a] Natural Drug Discovery Group, School of Pharmacy, Queen's University Belfast, Belfast BT9 7BL, Northern Ireland, UK
[b] China Medical University-The Queen's University of Belfast Joint College, No.77 Puhe Road, Shenyang North New Area, Shenyang 110122, PR China
[c] College of Traditional Chinese Medicine, Nanjing University of Chinese Medicine, Nanjing 210023, PR China

ARTICLE INFO

Keywords:
Antimicrobial peptide
Brevinin-1
Drug-resistant
LPS binding
DNA binding

ABSTRACT

Antimicrobial peptides (AMP) have emerged as promising candidates for addressing the clinical challenges posed by the rapid evolution of antibiotic-resistant microorganisms. Brevinins, a representative frog-derived AMP family, exhibited broad-spectrum antimicrobial activities, attacking great attentions in previous studies. However, their strong haemolytic activity and cytotoxicity, greatly limit their further development. In this work, we identified and characterised a novel brevinin-1 peptide, brevinin-1pl, from the skin secretions of the northern leopard frog, *Rana pipiens*. Like many brevinins, brevinin-1pl also displayed strong haemolytic activity, resulting in a lower therapeutic index. We employed several bioinformatics tools to analyse the structure and potential membrane interactions of brevinin-1pl, leading to a series of modifications. Among these analogues, des-Ala^{16}-[Lys^{4}]brevinin-1pl exhibited great enhanced therapeutic efficacy in both *in vitro* and *in vivo* tests, particularly against some antibiotics-resistant *Escherichia coli* strains. Mechanistic studies suggest that des-Ala^{16}-[Lys^{4}]brevinin-1pl may exert bactericidal effects through multiple mechanisms, including membrane disruption and DNA binding. Consequently, des-Ala^{16}-[Lys^{4}]brevinin-1pl holds promise as a candidate for the treatment of drug-resistant *Escherichia coli* infections.

1. Introduction

The escalating challenge of antimicrobial resistance (AMR) has significantly intensified the strain on the global healthcare sector and prompted the quest for innovative antimicrobials [1–4]. In contrast to conventional antibiotics, AMPs offer distinct advantages such as potent antibacterial activity, low cytotoxicity, and a reduced likelihood of inducing resistance, thus attracting considerable interest in recent decades [5–8]. In addition to their potent antimicrobial properties, many AMPs have been discovered to possess a variety of other bioactive functions, including antibiofilm activities, wound healing promotion, anticancer effects, and immunomodulatory activities [9–13]. The synergistic effects of AMPs in combination with conventional antibiotics, particularly in targeting both planktonic and biofilm-forming bacteria, have also been increasingly explored and reported in recent years [9,14]. Consequently, AMPs have attracted significant attention in research over the past few decades [15,16]. Among the diverse natural AMP sources, those derived from amphibians, particularly frogs, stand out due to their abundance and diversity [17–20]. As one of the representative families among frog-derived AMPs, brevinins, comprising brevinin-1 and brevinin-2 subfamilies, have been extensively explored and have demonstrated robust antimicrobial properties against a wide range of microorganisms [17,21,22]. Additionally, some of them exhibit great cytotoxic effects against various human cancer cells, positioning them as promising candidates for novel therapeutic agents [23–25]. However, their strong haemolytic activity and cytotoxicity towards human healthy cells greatly impede the further development [2,26]. Consequently, strategies aimed at controlling toxicity while preserving their bioactive functions have become heat-spot in current brevinin-1 modification works. To address the challenges of poor selectivity, biostability, and delivery of AMPs, a series of strategies have been developed based on structure-activity relationship studies, aiming to optimize AMP activity and enhance their proteolytic stability [11]. These strategies generally include the incorporation of D- or non-natural amino

* Corresponding authors.
E-mail addresses: jhu16@qub.ac.uk (J. Hu), w.pu@qub.ac.uk (W. Pu), yangyang.jiang@qub.ac.uk (Y. Jiang), t.wang@qub.ac.uk (T. Wang).
[1] These authors contributed equally to this work.

https://doi.org/10.1016/j.csbj.2024.09.006
Received 28 June 2024; Received in revised form 12 September 2024; Accepted 12 September 2024
Available online 19 September 2024

acids, truncations, PEGylation, lipidation, cyclisation, and various modifications aimed at improving delivery or reducing costs [10,11,27–29]. For example, truncation and amino acid substitution have effectively improved the therapeutic index of brevinin-1OS, leading to the development of a short derivative, OSf, with potent anti-MRSA activity in both *in vitro* and *ex vivo* tests [30]. Additionally, the introduction of D-amino acids has endowed the brevinin-1LTe analogue with effective antibacterial activity against both planktonic and biofilm cells in both *in vitro* and *in vivo* experiments [2].

In this study, we identified and characterised a novel brevinin-1 peptide, brevinin-1pl, from the skin secretion of the frog, *Rana pipiens*. Like most reported brevinin-1 peptides, brevinin-1pl exhibited potent antimicrobial activities against tested bacterial strains, but also induced strong haemolytic activity, resulting in a low therapeutic index. To address this issue, we employed a set of bioinformatics tools to analyse its structural features and predict potential interactions with mammalian membranes. Based on these predictions and previous experiences, we designed six analogues of brevinin-1pl aimed at reducing haemolysis while preserving antimicrobial functions. Among these analogues, des-Ala^{16}-[Lys^{4}]brevinin-1pl was successfully developed, demonstrating improved therapeutic efficacy and potent anti-*E. coli* activities against both antibiotic-sensitive and resistant strains. Des-Ala^{16}-[Lys^{4}]brevinin-1pl rapidly eradicates *E. coli* cells through a combination mode of action, as confirmed by *in vivo* anti-*E. coli* studies, which highlight its potential as a novel antimicrobial agent. In summary, the modification work in this study provides valuable insights into brevinin-1 peptide research and paves the way for further development of these peptides as novel antimicrobials. The promising anti-*E. coli* efficacy of des-Ala^{16}-[Lys^{4}] brevinin-1pl suggests its potential for advancement in future research endeavours.

2. Materials and methods

2.1. Collection of skin secretion from Rana pipiens

Skin secretions of *Rana pipiens* were collected from the dorsal skin as described previously [31]. The investigation adhered to the regulations outlined in the UK Animal (Scientific Procedures) Act of 1986, under project license PPL 2694, granted by the Department of Health, Social Services, and Public Safety in Northern Ireland. The procedures underwent evaluation by the IACUC of Queen's University Belfast and received approval on March 1st, 2011.

2.2. Molecular cloning of brevinin-1pl precursor encoding cDNA

Polyadenylated mRNA was isolated from the skin secretion suspension using a Dynabeads mRNA Direct Kit (Dynal Biotech, UK). A SMART-RACE kit (Clontech, UK) was utilised to acquire the DNA sequence of prepro-peptide nucleic acids using a NUP primer (supplied with the kit) and a degenerate sense primer (S1; 5' -GAWYYAYYHRAGCCYAAA-DATG-3') [32]. The PCR products were purified, cloned using a pGEM-T vector (Promega, USA), and sequenced by a commercial service provided by Eurofins (Eurofins Biosearch, Belfast, UK).

2.3. Bioinformatics analysis

National Center for Biotechnology Information (NCBI) - Basic Local Alignment Search Tool (BLAST) was used to analyse the identified peptide. Jalview program is employed to perform the multiple sequence alignment analysis. The secondary structures of peptides were predicted using the online server PEPFOLD3 (https://bioserv.rpbs.univ-paris-diderot.fr/services/PEP-FOLD3/) [33]. The helical wheel diagrams of peptides were generated using the HeliQuest server (https://heliquest.ipmc.cnrs.fr/) [34]. PPM 3.0 web server was utilised to calculate the possible binding model and membrane affinity of peptides (https://opm.phar.umich.edu/ppm_server3_cgopm) [35]. PyMOL program was employed to virtualise the prediction results. The molecular docking of the peptide with the DNA molecule was performed using the online server HDOCK [36]. The predicted structure model of the peptide obtained from the PEPFOLD3 server was submitted as the ligand, while the crystal structure of B-DNA (PDB: 1BNA) was set as the receptor. HDOCK, which employs a combined template-based and template-free algorithm, was used for automatic molecular-level protein–DNA docking. The top result was selected for further analysis using the Protein-Ligand Interaction Profiler (PLIP) web tool [37].

2.4. Peptide synthesis and characterisation

Peptides used in this work were synthesised with the solid phase peptide synthesis strategy (SPPS) using a tribute peptide synthesiser machine (Gyros Protein Technology, USA). All synthetic peptides were then oxidised by dimethyl sulfoxide (DMSO) to formed disulphide bridge [38] and purified with a reverse-phase HPLC (RP-HPLC) system (Waters, UK) equipped with an Aeris Peptide XB-C18 HPLC Column (250 ×21.2 mm, 5 μm, Phenomenex, UK). The purified peptides were further characterised with a MALDI-TOF mass spectrometry (4800 MALDI TOF/TOF, Applied Biosystems, USA).

2.5. Secondary structure analysis

The secondary structure of peptides was determined using circular dichroism (CD) spectrometry (J-815, Jasco, UK). Peptides (final concentration 50 μM) were prepared in 10 mM Ammonium acetate (NH_4AC) for mimicking aqueous environments and in 50 % TFE (v/v, in 10 mM NH_4AC) for mimicking membrane-like environments. Wavelength detection ranged from 190 nm to 260 nm with a scanning speed of 100 nm/min. The bandwidth and data pitch used were 1 nm and 0.5 nm, respectively. Additionally, changes in the conformations of brevinin-1pl and brevinin-1pl-del 16 in water and in the presence of LPS were monitored using CD spectrometry. LPS (O26:B6, 100 μM, Sigma-Aldrich, UK) was added to the 10 mM NH_4AC solution to prepare the Lipopolysaccharides (LPS) environment. To analyse the interaction of the peptide with plasmid DNA, DNA samples (10 μg/ml) were tested with and without various ratios of peptides. The analysis was conducted by measuring the absorbance from 360 nm down to 230 nm [39,40]. The K2D3 server was utilised to analyse the possible secondary structure contents of peptides in different environments (https://cbdm-01.zdv.uni-mainz.de/~andrade/k2d3/) [41].

2.6. Antimicrobial assays

The antimicrobial activities of peptides were assessed by determining their minimal inhibitory concentration (MIC) and minimal bactericidal concentration (MBC) values, following established protocols [42]. The assay involved testing against three Gram-positive bacteria: *Staphylococcus aureus* NCTC 10788 (*S. aureus* 10788), Methicillin-resistant *Staphylococcus aureus* NCTC 12493 (MRSA 12493), and *Enterococcus faecalis* NCTC 12697 (*E. faecalis* 12697); five Gram-negative bacteria: *Escherichia coli* ATCC 8739 (*E. coli* 8739), *E. coli* NCTC 13846 (*E. coli* 13846), *E. coli* BAA 2340 (*E. coli* 2340), *Pseudomonas aeruginosa* ATCC CRM 9027 (*P. aeruginosa* 9027), *Klebsiella pneumoniae* ATCC 43816 (*K. pneumoniae* 438416), and *Acinetobacter baumannii* BAA 747 (*A. baumannii* 747); and one yeast strain, *Candida albicans* ATCC 10231 (*C. albicans* 10231). Each experiment was conducted with three independent repetitions, each consisting of three replicates. Bacteria/yeast were inoculated for 16–18 h and then subcultured in 20 ml fresh medium until the optical density (OD) of the cultures at 550 nm reached 0.23 (for tested Gram-positive bacteria), 0.4 (for tested Gram-negative bacteria), and 0.15 (for tested yeast strain), corresponding to the density of 1×10^8 colony-forming units (cfu)/ml for the bacteria, and 1×10^6 cfu/ml for the yeast. Afterwards, the cultures were diluted to a final density of 5×10^5 cfu/ml and incubated

with peptide solutions at concentrations ranging from 1 to 128 μM. The plates were incubated at 37 °C for 18 h, and bacterial/yeast growth was determined by measuring absorbance values at 550 nm using a Synergy HT plate reader (Bio Tek, USA). MIC results were defined as the lowest concentration of peptide at which no observed growth of microorganisms could be detected. For the MBC assay, the culture in each well was spotted onto an agar plate and incubated at 37 °C for 18 h. The MBC results were defined as the lowest concentration of peptide at which no colony was observed. The experiment was conducted independently in three separate sessions, with each experiment performed in triplicate. The geometric mean of the MICs for the tested peptides was calculated using the online tool Alcula (http://www.alcula.com/calculators/statistics/geometric-mean/).

2.7. Haemolysis assay

The haemolytic activity of peptides was evaluated using the horse erythrocytes as described previously [43]. In short, peptide solutions (final concentrations ranging from 1 μM to 128 μM) were incubated with 2 % horse erythrocytes (E&O LABORATORIES LIMITED, UK) at 37 °C for 2 h. Triton x-100 (1 %, Sigma-Aldrich, UK) was used as the positive control group, and the sterile PBS was set as the blank group. After that, the peptide-horse erythrocytes mixture was centrifuged at 930g for 10 min, and the absorbance at 570 nm of the supernatant was measured. The percentage haemolysis was calculated using the formal:

Percentage Haemolysis= (Abs $_{Sample}$-Abs $_{Blank}$)/ (Abs $_{Positive}$-Abs $_{Blank}$) × 100 %.

The experiment was performed in triplicated, with each trial conducted independently.

2.8. Salt sensitivity assay

The sensitivity of peptides to various ions was assessed by measuring changes in their MIC and MBC values. Seven types of ions, including 150 mM NaCl, 4.5 mM KCl, 2 mM $CaCl_2$, 1 mM $MgCl_2$, 8 μM $ZnCl_2$, 6 μM NH_4Cl, and 4 μM $FeCl_3$, were introduced into the Mueller-Hinton broth (MHB) medium during the antimicrobial assays [42]. Each experiment was independently repeated three times.

2.9. Time-killing kinetic assay

The rate of sterilisation was assessed using time-killing kinetics assay. Diluted bacterial suspensions (10^6 CFU/ml) were mixed with appropriate peptide concentrations (1 × MIC, 2 × MIC, and 4 × MIC). Ten microliters of the mixture suspended in PBS solution were sampled at different time intervals (0 min, 5 min, 10 min, 20 min, 30 min, 60 min, 90 min, 120 min, and 180 min) and plated onto agar plates. After 24 h of incubation, the number of bacterial colonies was counted. The experiment was conducted independently in three separate sessions, with three replications of each experiment performed.

2.10. LPS binding assay

Lipopolysaccharide (LPS) binding capacity of antimicrobial peptides was assessed using the fluorescent dye, BODIPY™ TR Cadaverine (BC, ThermoFisher, USA). Initially, 50 μg/ml LPS solution and 5 μg/ml BC dye solution were prepared by dilution with Tris-HCl buffer. After standing at room temperature for 4 h, equal volumes of the mixture were mixed with peptide solutions (concentrations ranging from 2 μM to 32 μM) and added to the wells of the black plate, resulting in final concentrations of 25 μg/ml LPS and 2.5 μg/ml BC dye. The plate was then incubated at 37 °C for 1 h, and fluorescence was measured using a Synergy HT plate reader (BioTek, USA) with excitation and emission wavelengths set at λ = 590 nm and λ = 645 nm, respectively. The experiment was conducted independently in three separate sessions, with three replications of each experiment performed.

2.11. NPN assay

The NPN assay was conducted to assess the outer membrane (OM) permeabilisation activity of peptides [44]. Bacteria in the logarithmic growth phase were centrifuged at 3000g for 10 min to remove the supernatant, and the pellet was washed three times with HEPES buffer (5 mM, pH 7.2, containing 5 mM glucose). Subsequently, the bacterial suspension was diluted in the prepared HEPES buffer to a density of 1 × 10^7 CFU/ml and mixed with peptide solutions (1 × MIC, 2 × MIC, 4 × MIC) and NPN solutions (Sigma-Aldrich, UK). The mixture was then incubated at 37 °C for 2 h. The fluorescent intensity of NPN was measured at wavelengths of 420 nm (excitation) and 350 nm (emission). Melittin served as the positive control (100 % permeability rate), while HEPES buffer served as the negative control (0 % permeability rate). The experiments were conducted in three independent runs.

2.12. SYTOX green assay

SYTOX green assay was conducted to evaluate the cytoplasmic membrane permeabilisation activity of peptides as describe previously [25]. In short, bacteria in log phase were centrifuged to remove the supernatant, and the cell pellets were washed three times with 5 % TSB buffer (prepared in 0.85 % NaCl). Following the final centrifugation, the bacterial cell pellets were re-suspended in the 5 %TBS to a density of OD_{590} = 0.7. Diluted bacterial suspension was then mixed with peptide solutions (1 × MIC, 2 × MIC, 4 × MIC) and incubated at 37 °C for 2 h. After incubation, diluted SYTOX green-fluorescent nucleic acid stain (final concentration 50 μM, ThermoFisher, USA) was added to the mixture, and the fluorescent intensity was detected at an excitation wavelength of 360 nm and an emission wavelength of 460 nm. The experiments run in three independent repeats with three replicates each time.

2.13. ONPG assay

The ONPG assay was conducted to further assess the membrane permeabilisation activity of peptides against the tested *E. coli* strains [45,46]. *E. coli* cells cultured in LB medium (containing 2 % lactose) were incubated until reaching the logarithmic phase and then centrifuged to discard the supernatant. The bacterial cell pellets were suspended to a density of OD_{600} = 0.5 and then ten-fold diluted in a PBS buffer containing 1.5 mM ONPG (Sigma-Aldrich, UK) at a pH of 7.4. The diluted bacterial suspension was subsequently incubated with peptide solutions. The changes in absorbance were dynamically monitored at 37 °C with a wavelength of 460 nm. The experiments were independently repeated three times with three replicates each time.

2.14. DNA binding assay

Gel retardation experiments were conducted to study the potential interactions of brevinin-1pl and des-Ala^{16}-[Lys^4]brevinin-1pl with *E. coli* plasmid DNA. Briefly, peptide solutions (final concentrations ranging from 1 μM to 32 μM) were incubated with *E. coli* plasmid DNA (100 ng, Sigma-Aldrich, UK) in a sample buffer containing 1 mM EDTA, 10 mM Tris-HCl (pH 8.0), 5 % glucose, 50 μg/ml BSA, and 20 mM KCl. After incubation at 37 °C for 1 h, the mixture was analysed by agarose gel electrophoresis in 1 × TAE buffer (ITW REAGENTS, UK) [47–49]. Equal concentrations of the DNA-binding peptide Buforin II were used as the control group [47,50].

2.15. In vivo antibacterial study

The *in vivo* anti-*E. coli* activities of peptides brevinin-1pl and des-Ala^{16}-[Lys^4]brevinin-1pl were evaluated using the *Galleria mellonella* (*G. mellonella*) larvae model [2,42,51]. Initially, larvae were infected with *E. coli* cells by injecting a suspension (1 × 10^7 CFU/ml) into the last

right proleg for 1 h. Subsequently, peptide solutions at doses of 10 mg/kg, 20 mg/kg, and 40 mg/kg (equal to 1 × MIC, 2 × MIC, and 4 × MIC of the brevinin-1pl-del 16) were administered to treat the infected larvae. All larvae were then cultivated at 37 °C for five days, and survival rates were assessed daily, with each group consisting of ten larvae. Rifampin (20 mg/kg, Sigma-Aldrich, UK) served as the positive control group, while the negative control group involved treating infected larvae with the same volume of sterile PBS. Each experiment was independently conducted three times.

2.16. MTT assay

Two human cancer cell lines, non-small-cell lung cancer line H838 (ATCC, USA) and human breast cancer cell line MCF-7 (ATCC, USA), and one human healthy cell line, human keratinocytes cell HaCaT (Caltag Medsystems, UK) were employed to assess the cytotoxic activity of Brevinin-1pl and its analogues using the MTT assay. H838 cells were cultured in RPMI-1640 medium (Gibco, UK), while MCF-7 and HaCaT cells were cultured in DMEM medium (Gibco, UK), both supplemented with 10 % (v/v) fetal bovine serum (FBS, Gibco, UK) and 1 % (v/v)

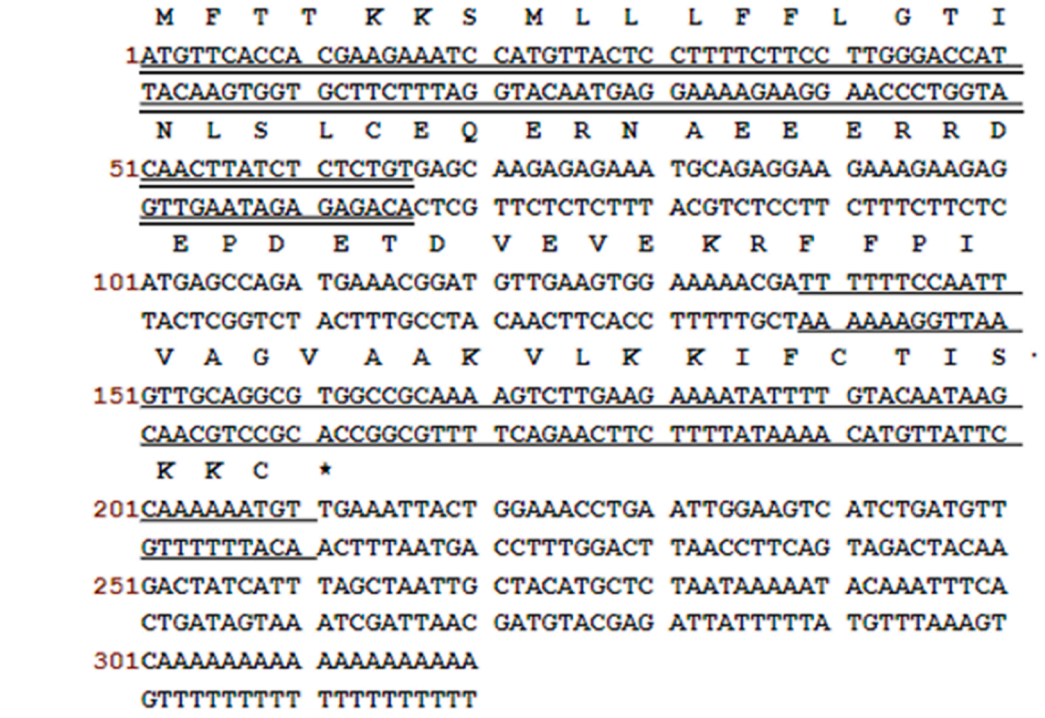

(a)

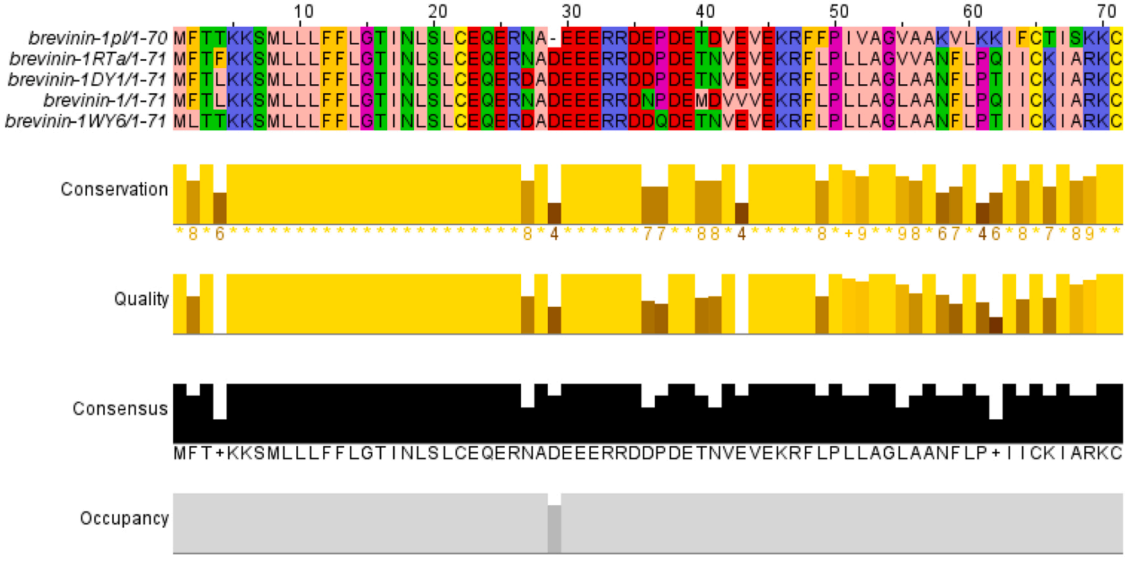

(b)

Fig. 1. (a) Brevinin-1pl precursor cDNA and corresponding amino acid sequence. The nucleotide sequence of signal peptide is labelled with double-underline, and the nucleotide sequence of the deduced mature peptide sequence is labelled with single-underline. The asterisk represents the stop code. (b) Multiple sequence alignment results of brevinin-1pl with similar peptides found in NCBI-BLAST database. Zappo colour scheme is used to label and reveal patterns of variations.

penicillin–streptomycin (PS, Gibco, UK). Cells were seeded in 96-well plates at a density of 8000 cells per well for H838 and MCF-7 and 10,000 cells for HaCaT and incubated overnight at 37 °C with 5 % CO_2 until attached. After attachment, the cells were treated with peptide solutions (final concentrations ranging from 10^{-4} M to 10^{-9} M). After 22 h of exposure, MTT solution (final concentration 0.5 mg/ml) was added to each well and incubated at 37 °C for 4 h. Subsequently, the medium was removed, and 100 µl of DMSO was added to each well. After shaking for 15 min in a shaking incubator, the absorbance was measured at a wavelength of 570 nm using a Synergy HT plate reader.

2.17. Statistical analysis

Experiment data in this work was analysed using the GraphPad Prism 9.0 software (GraphPad Software Inc., San Diego, CA, USA), and the results are represented as standard error of the mean (S.E.M.). Significance levels were determined through one-way ANOVA tests, comparing the mean values of the designated data sets. Asterisks denote significant differences (* $p \leq 0.05$; ** $p < 0.01$; *** $p < 0.001$; **** $p < 0.0001$).

3. Results

3.1. Molecular cloning and characterisation of brevinin-1pl precursor cDNA

The cDNA encoding an AMP precursor was obtained through molecular cloning (Fig. 1a). The cDNA consists of 320 base pairs (bp) coding for 71 amino acids, including a signal peptide, acidic spacer, enzyme cleavage site (-KR-) and a putative mature peptide (FFPIVAGVAAKVLKKIFCTISKKC). The amino acid sequence of this prepropeptide was then submitted and analysed with BLASTp program. As shown in Fig. 1b, the identified peptide shared high similarity with peptides in brevinin-1 family, indicating that this peptide may be a novel brevinin-1 peptide. Therefore, it was named brevinin-1pl. The nucleotide sequence of brevinin-1pl precursor was deposited in GenBank with an accession number of PP898169.

3.2. Secondary structure predication and modification of brevinin-1pl

The prediction result from PEPFOLD 3 server demostrated that brevinin-1pl may adopt high degree of helicity in its secondary structure (Fig. 2a and b), with an integrated hydrophobic face consisting of nine hydrophobic residues (Fig. 2c). Brevinin-1 peptides typically

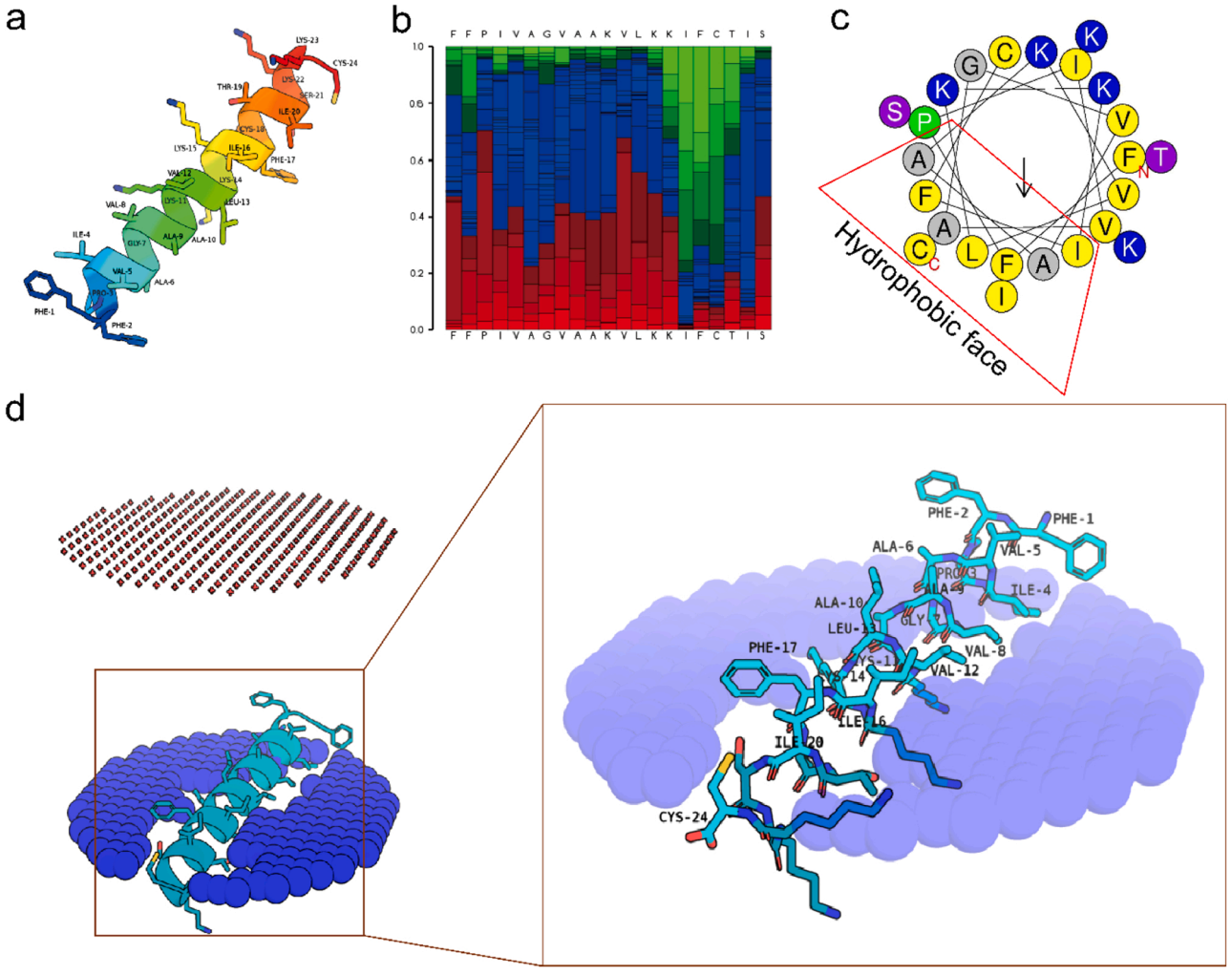

Fig. 2. (a) Predicted secondary structure of breinin-1pl. (b) Distribution of predicted secondary structure in residues. Red, blue and green represents possible distribution of helical, coil and extended structure, respectively. (c) Helical wheel diagram of possible helix part of brevinin-1pl. The hydrophobic face calculated by the HeliQuest server is labelled in red. (d) Possible binding mode of brevinin-1pl with the plasma membrane (mammalian) model (Red represents the extracellular side; blue represents the intracellular side) predicted by PPM server and virtualised in PyMOL program. Residues embedded in the membrane are labelled with three-letter code.

demonstrate potent antimicrobial activities against a broad spectrum of microorganisms. However, their high toxicity has significantly hindered their advancement as novel antimicrobials. Hence, the binding mode of brevinin-1pl with mammalian plasma membrane was analysed using the PPM server. The predicted results revealed that the peptide's maximal penetration depth is 9.2 ± 2.0 Å, and residues at positions 1–14, 16–17, 20, and 24 may play crucial roles in embedding the peptides in the plasma membrane.

The high degree of helicity and potential strong binding affinity with the mammalian membrane may enable brevinin-1pl to exhibit remarkable cytotoxicity, similar to many reported brevinin-1 peptides. Therefore, based on the prediction results, modifications to brevinin-1pl were carried out to preserve its antimicrobial functions while decreasing its toxicity. Firstly, we substituted the 4th Ile with Lys to design [Lys^4] brevinin-1pl. Building upon [Lys^4]brevinin-1pl, further modifications focused on the 13th Leu and 16th Ile sites. They were replaced with weaker hydrophobic amino acid Ala (resulting in analogues [Lys^4, Ala^{13}]brevinin-1pl, [Lys^4, Ala^{16}]brevinin-1pl, and [Lys^4, Ala^{13,16}]brevinin-1pl) or deleted (yielding analogues des-Ala^{16}-[Lys^4]brevinin-1pl and des-Leu^{13}, Ala^{16}-[Lys^4]brevinin-1pl) to control hydrophobicity (Table 1) and reduce their potential binding capacity with mammalian membranes. MALDI-TOF MS results demonstrated that all peptides used in the test were successfully synthesized, oxidized, and purified (Fig. S1). HPLC results indicated that all synthetic peptides were purified to achieve a purity of over 90 % (Figs. S2). The detected mass of the peptides matches the theoretical mass, indicating successful disulfide bond formation.

3.3. Secondary structure analysis of brevinin-1pl and its analogues

The secondary structure of brevinin-1pl and its analogues was analysed using CD spectroscopy (Fig. 3). In the 10 mM NH_4AC solution, all peptides primarily adopt a random coil structure, while they mainly adopt alpha-helix, anti-parallel, and parallel structures in the 50 % TFE solution (Table 2). The introduction of Lys or Ala replacements produced great effects on the percentage of the α helix content of peptide [Lys^4]brevinin-1pl, [Lys^4, Ala^{13}]brevinin-1pl, [Lys^4, Ala^{16}]brevinin-1pl and [Lys^4, Ala^{13,16}]brevinin-1pl in NH_4AC solution while do not remarkably affect the α helix formation in the TFE solution. However, their contents of anti-parallel structures slightly decreased, while the parallel structure contents slightly increased. In contrast, for des-Ala^{16}-[Lys^4]brevinin-1pl and des-Leu^{13}, Ala^{16}-[Lys^4]brevinin-1pl, the removal of the 16th and 13th residues improved the helix content of the peptide.

3.4. Antimicrobial activities and therapeutic index values of brevinin-1pl and its analogues

Brevinin-1pl exhibited potent antibacterial activities against the tested bacterial strains, with MIC values ranging from 2 to 8 μM (Table 3). Among the tested bacterial strains, Gram-positive bacteria were more susceptible to brevinin-1pl, with a GM value of 2.52 μM. However, no obvious inhibitory activity against the tested yeast strain, *C. albicans* 10,231, was observed with brevinin-1pl. Brevinin-1pl displayed strong haemolytic activity toward horse erythrocytes, with an HC_{10} value of 8.28 μM, contributing to its low TI values (TI_{G+} = 3.29 and TI_{G-} = 1.46) (Table 4). Simply replacing the 4th Ile with Lys, although producing no obvious effects on the TI values of brevinin-1pl-6k, alleviated its haemolytic activity. Its HC_{10} value increased from 8.28 μM to 13.68 μM, and the HC_{50} value increased from 37.64 μM to 80.77 μM. Introducing Ala at the 13th and 16th positions did not help improve the TI values of brevinin-1pl-13A and brevinin-1pl-16A. However, the removal of the 16th Ile, although affecting the antibacterial activity against tested Gram-positive bacteria remarkably, decreased the haemolysis of brevinin-1pl-del 16, resulting in a TI_{G-} value of 55.77, much higher than that of brevinin-1pl and other analogues. Especially, its TI value against *E. coli* 8739 is 128, indicating potential efficacy against *E. coli* strains. Further removal of the 13th Ala greatly affected the antibacterial activities of breinin-1pl-del 13, 16 and reduced the TI values against tested bacteria.

3.5. Antibacterial activities of brevinin-1pl and des-Ala^{16}-[Lys^4]brevinin-1plagainst drug-resistant E. coli

Breinin-1pl and its analogues showed relatively stronger antimicrobial effects on the tested *E. coli* strain. Meanwhile, among designed analogues, des-Ala^{16}-[Lys^4]brevinin-1pl exhibited the highest TI values. Therefore, both the parent peptide brevinin-1pl and the analogue des-Ala^{16}-[Lys^4]brevinin-1plwere selected to evaluate their effects on two drug-resistant *E. coli* strains. As shown in Table 5, both peptides exhibited potent antibacterial activities against the tested *E. coli* strains. Des-Ala^{16}-[Lys^4]brevinin-1pl displayed higher anti-*E. coli* efficacy with a TI value of 80.63, much higher than that of the parent peptide breinin-1pl.

3.6. Salt sensitivity of brevinin-1pl and des-Ala^{16}-[Lys^4]brevinin-1pl

The sensitivity of brevinin-1pl and des-Ala^{16}-[Lys^4]brevinin-1pl to different salt environments was assessed by measuring changes in their MIC and MBC values against three *E. coli* strains. As indicated in Table 6, the presence of calcium and magnesium ions significantly impacted the antibacterial activities of both peptides, resulting in MIC/MBC value increases ranging from two-fold to sixteen-fold. Des-Ala^{16}-[Lys^4]brevinin-1pl exhibited enhanced tolerance to sodium ions compared to the parent peptide.

3.7. Time-killing kinetics study of brevinin-1pl and des-Ala^{16}-[Lys^4] brevinin-1pl

The time-killing kinetics of brevinin-1pl and its analogue des-Ala^{16}-[Lys^4]brevinin-1pl were assessed on three *E. coli* strains. Both peptides demonstrated a rapid killing rate against the tested *E. coli* strains, eradicating all cells within 60 min (Fig. 4). However, des-Ala^{16}-[Lys^4] brevinin-1pl exhibited significantly higher efficiency in killing all tested *E. coli* strains compared to brevinin-1pl, completely eradicating cells within 10 min. Remarkably, at a concentration of 4 × MIC, des-Ala^{16}-[Lys^4]brevinin-1pl was capable of almost immediate bacteria eradication upon contact.

Table 1
Partial structural parameters of brevinin-1pl and its analogues.

Peptide name	Sequence	Theoretical molecular Weight	Net charge	Hydrophobicity <H>	Hydrophobic moment < μH>
brevinin−1pl	FFPIVAGVAAKVLKKIFCTISKKC	2609	5	0.765	0.447
[Lys^4]brevinin−1pl	FFPKVAGVAAKVLKKIFCTISKKC	2624	6	0.601	0.567
[Lys^4, Ala^{13}]brevinin−1pl	FFPKVAGVAAKVAKKIFCTISKKC	2581	6	0.519	0.504
[Lys^4, Ala^{16}]brevinin−1pl	FFPKVAGVAAKVLKKAFCTISKKC	2581	6	0.514	0.487
[Lys^4, Ala$^{13,\ 16}$]brevinin−1pl	FFPKVAGVAAKVAKKAFCTISKKC	2539	6	0.432	0.421
des-Ala^{16}-[Lys^4]brevinin−1pl	FFPKVAGVAAKVLKK_FCTISKKC	2510	6	0.526	0.587
des-Leu^{13}, Ala^{16}-[Lys^4] brevinin−1pl	FFPKVAGVAAKV_KK_FCTISKKC	2397	6	0.448	0.426

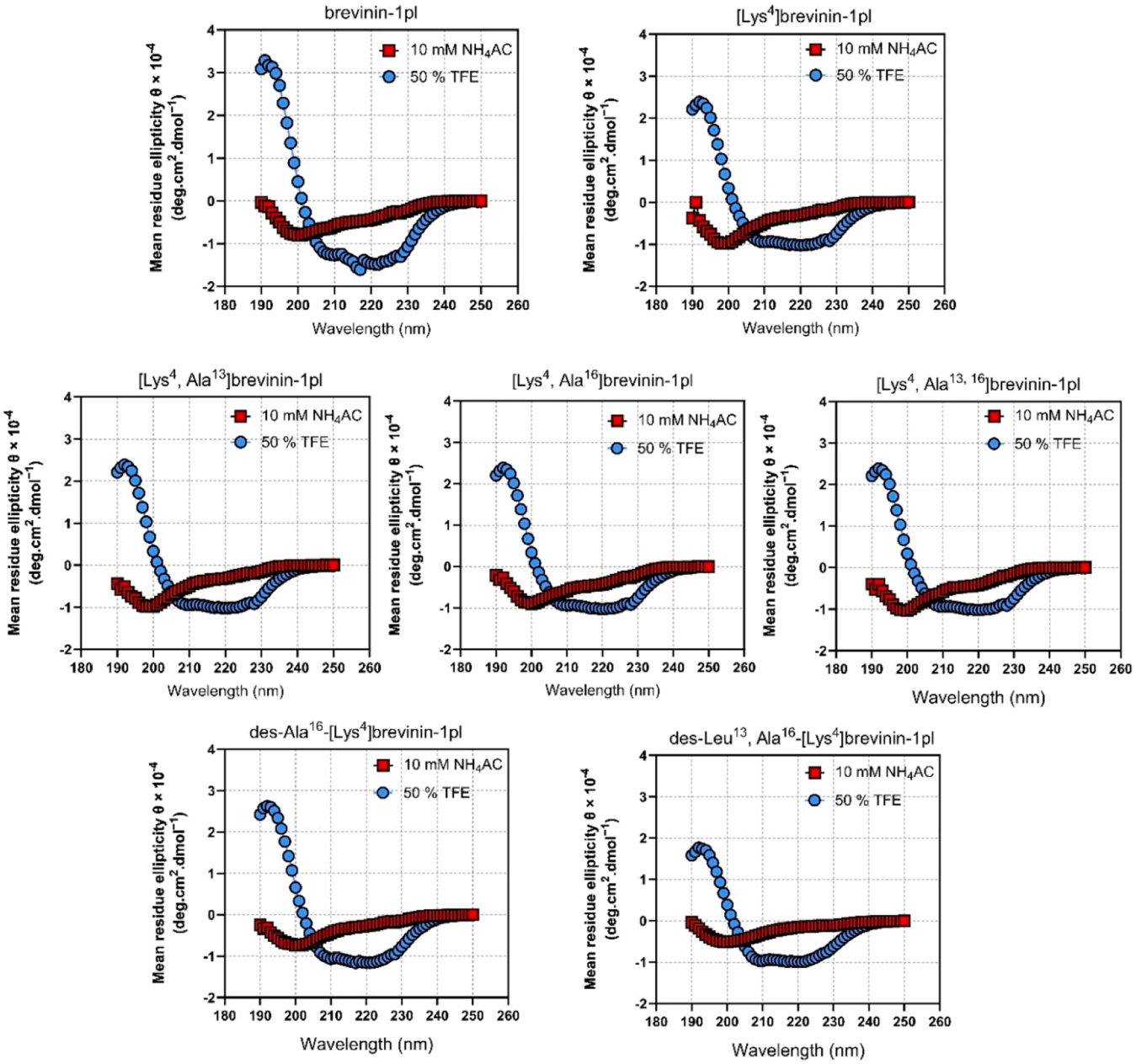

Fig. 3. CD spectra of brevinin-1pl and its analogues. The red line represents the results of peptides in 10 mM NH_4AC solution. The blue line represents the results of peptides in 50 % TFE buffer.

Table 2
Estimated α helix structure content (%) of brevinin-1pl and its analogues.

Peptide	α helix (%)	
	NH_4AC	TFE
brevinin−1pl	61.78	95.4
[Lys^4]brevinin−1pl	26.82	95.4
[Lys^4, Ala^{13}]brevinin−1pl	18.26	95.4
[Lys^4, Ala^{16}]brevinin−1pl	44.15	95.4
[Lys^4, $Ala^{13, 16}$]brevinin−1pl	31.17	95.4
des-Ala^{16}-[Lys^4]brevinin−1pl	31.95	95.28
des-Leu^{13}, Ala^{16}-[Lys^4]brevinin−1pl	34.65	95.28

3.8. Anti-E. coli mechanism studies of brevinin-1pl and des-Ala^{16}-[Lys^4] brevinin-1pl

To investigate the antibacterial mechanisms of brevinin-1pl and des-Ala^{16}-[Lys^4]brevinin-1pl against the tested *E. coli* strains, a series of experiments were conducted. Firstly, the interaction capacity of brevinin-1pl and des-Ala^{16}-[Lys^4]brevinin-1pl with LPS was studied (Fig. 5a). Compared to the control peptide Melittin, both peptides exhibited a more potent binding ability with LPS. In particular, the analogue des-Ala^{16}-[Lys^4]brevinin-1pl showed the strongest binding affinity with LPS among the tested peptides. The EC50 value of des-Ala^{16}-[Lys^4]brevinin-1pl is around 0.65 μM, which is lower than 0.77 μM for brevinin-1pl and 0.93 μM for melittin. The binding affinity peaked at 2 μM for all three peptides. Meanwhile, the CD spectra results showed that the presence of LPS altered the conformation of brevinin-1pl and des-Ala^{16}-[Lys^4]brevinin-1pl in an aqueous environment, as evidenced by obvious negative peaks observed at around 208 nm and 220 nm (Fig. 5b). According to the K2D3 prediction, in the presence of LPS, the α helix content of brevinin-1pl and des-Ala^{16}-[Lys^4]brevinin-1pl was increased to 95.09 % and 95.44 %, respectively.

Table 3
Antimicrobial screening results of brevinin-1pl and its analogues. MICs/MBCs (μM) values are listed.

Strains	*S. aureus* 6538	MRSA 12,493	*E. faecium* 12,697	*E. coli* 8739	*K. pneumoniae* 43,816	*P. aeruginosa* 9027	*A. baumannii* 747	*C. albicans* 10,231
brevinin−1pl	2 / 2	2 /2	4 / 4	4 / 4	8/8	8/16	8/16	> 128
[Lys^4]brevinin−1pl	4/ 4	4/ 4	16 / 16	4 / 4	8/8	8/8	16/16	> 128
[Lys^4, Ala^{13}]brevinin−1pl	4/ 4	4/ 4	128/128	4 / 4	8/8	8/8	16/16	32/128
[Lys^4, Ala^{16}]brevinin−1pl	4/ 4	4 /4	32/64	4 / 4	8/8	8/8	8/8	32/64
[Lys^4, Ala^{13,16}]brevinin−1pl	16/16	8/ 8	> 128	8/ 8	16/16	32/32	32/32	32/64
des-Ala^{16}-[Lys^4] brevinin−1pl	32/32	> 128	64/> 128	2 /2	4/8	16/16	16/16	16/32
des-Leu^{13}, Ala^{16}-[Lys^4] brevinin−1pl	> 128	> 128	> 128	32/32	> 128	> 128	> 128	> 128

Table 4
HC_{10}, HC_{50}, Geometric Mean (GM), and TI values of brevinin-1pl and its analogues.

Treatments	HC_{10} (μM)	HC_{50} (μM)	GM (μM)		TI*		
			G+	G-	G+	G-	*E. coli* 8739
brevinin−1pl	8.28	37.64	2.52	5.66	3.29	1.46	2.07
[Lys^4]brevinin−1pl	13.68	80.77	6.35	8	2.15	1.71	3.42
[Lys^4, Ala^{13}]brevinin−1pl	4.59	41.34	12.7	8	0.36	0.57	1.15
[Lys^4, Ala^{16}]brevinin−1pl	2.51	84.86	8	5.66	0.31	0.44	0.63
[Lys^4, Ala$^{13,\ 16}$]brevinin−1pl	62.21	> 128	32	16	1.94	3.89	7.78
des-Ala^{16}-[Lys^4]brevinin−1pl	> 128	> 128	80.63	4.59	3.17	55.77	128
des-Leu^{13}, Ala^{16}-[Lys^4]brevinin−1pl	116.3	> 128	256	128	0.45	0.91	3.63

* TI value was calculated as HC_{10}/GM. When the HC_{10} value was over 128 μM, 256 μM was utilised to calculate the TI value. TI_{G+} and TI_{G-} represent the TI values of peptides against the tested Gram-positive and Gram-negative bacteria, respectively.

Table 5
MICs/MBCs (μM) and TI values of tested *E. coli* strains of brevinin-1pl and des-Ala^{16}-[Lys^4]brevinin-1pl.

Strain	*E. coli* 8739	*E. coli* 13846	*E. coli* 2340	TI
Description	(sensitive)	(mcr-1 positive)	(*bla*$_{KPC}$ positive)	
brevinin−1pl	4 / 4	4 / 4	4 / 4	2.07
des-Ala^{16}-[Lys^4] brevinin−1pl	2 /2	4 / 4	4 / 4	80.63

To assess the impact of brevinin-1pl and des-Ala^{16}-[Lys^4]brevinin-1pl on the *E. coli* membrane, we employed the NPN assay and SYTOX green assay. Additionally, the ONPG assay was utilised to further verify the membrane-disruptive effects of the peptides. For brevinin-1pl, its presence induced outer membrane permeabilisation of the three tested *E. coli* strains in a concentration-dependent manner (Fig. 6). The combined results of ONPG and SYTOX green assays indicated that brevinin-1pl greatly increased intracellular membrane permeability. Therefore, its anti-*E. coli* mechanism is more likely membrane-disruptive, similar to many reported AMPs. However, for the analogue des-Ala^{16}-[Lys^4]brevinin-1pl, the mode of action might be different. Firstly, the treatment of des-Ala^{16}-[Lys^4]brevinin-1pl did not induce significant changes in the outer membrane permeabilisation of the tested *E. coli* strains. Meanwhile, its impact on intracellular membrane permeabilisation was not concentration dependent. Although for *E. coli* 8739, it showed a concentration-dependent manner in the SYTOX green assay, it did not induce obvious changes in OD values in the ONPG assay, reflecting the low release of cytoplasmic beta-galactosidase. Taking these results into consideration, given the relatively fewer changes in the permeability of the membrane and the markedly different ultra-fast bactericidal efficiency, we suspect that des-Ala^{16}-[Lys^4]brevinin-1pl may affect bacterial targets beyond just the membrane, potentially involving some intracellular targets. Therefore, its interactions with *E. coli* DNA were studied.

As shown in Fig. 7a, the peptide des-Ala^{16}-[Lys^4]brevinin-1pl can interact with DNA molecules and retard their movement in electrophoresis. Complete retardation was observed at a concentration of 16 μM. In comparison, the DNA-binding peptide buforin II did not show complete retardation even at the highest tested concentration (64 μM). CD spectra were utilised to further verify the interaction of des-Ala^{16}-[Lys^4]brevinin-1pl with plasmid DNA. Both des-Ala^{16}-[Lys^4]brevinin-1pl and buforin II induced bending in the plasmid DNA (Fig. 7b). With gradual increases in the peptide ratio, there was a red shift of the maximum from 275 nm to 285 nm, accompanied by a decrease in peak ellipticity. This observation suggests that the peptides may interact with the base-stacking, thereby leading to changes in the DNA conformation. The Δε for buforin II increases at a relatively lower rate beyond the ratio

Table 6
MICs and MBCs values of brevinin-1pl and des-Ala^{16}-[Lys^4]brevinin-1plin different salt environments.

Strain	*E. coli* 8739		*E. coli* 13846		*E. coli* 2340	
Peptide	brevinin-1pl	des-Ala^{16}-[Lys^4]brevinin-1pl	brevinin-1pl	des-Ala^{16}-[Lys^4]brevinin-1pl	brevinin-1pl	des-Ala^{16}-[Lys^4]brevinin-1pl
Control	4 /4	2 /2	4 /4	4 /4	4 /4	4 /4
150 mM NaCl	16 /16	4 /4	8 /8	4 /8	4 /4	4 /4
4.5 mM KCl	4 /4	2 /2	8 /8	8 /8	4 /4	2 /2
2 mM $CaCl_2$	8 /8	8 /8	32 /64	64 /64	16 /16	16 /16
1 mM $MgCl_2$	16 /16	32 /32	16 /16	16 /16	8 /8	8 /8
8 μM $ZnCl_2$	4 /4	2 /2	8 /8	8 /8	4 /4	4 /4
6 μM NH_4Cl	4 /4	2 /2	8 /8	8 /8	4 /4	4 /4
4 μM $FeCl_3$	4 /4	2 /2	8 /8	8 /8	4 /4	4 /4

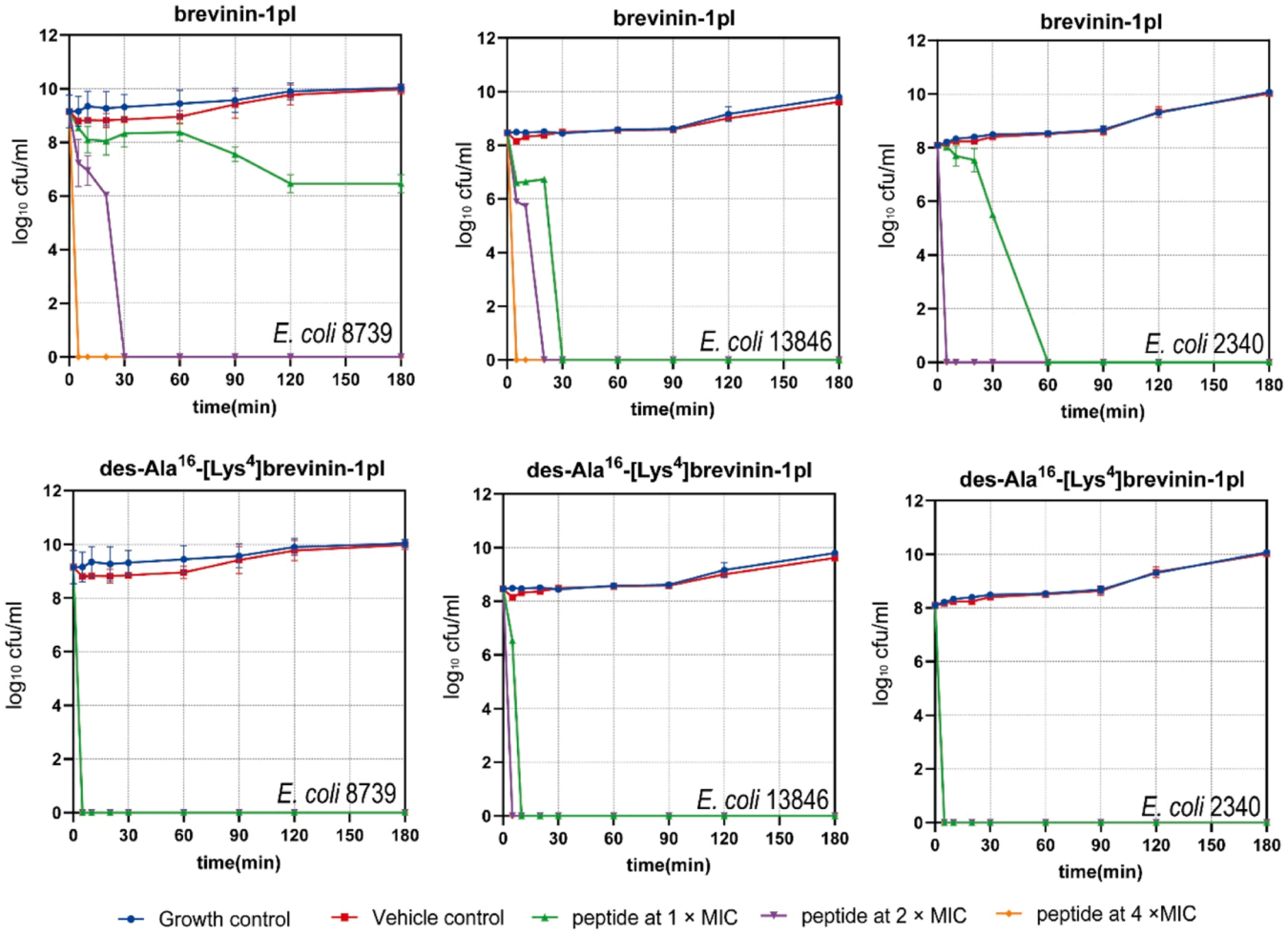

Fig. 4. Time-killing kinetic curves of brevinin-1pl (a) and des-Ala^{16}-[Lys^{4}]brevinin-1pl (b) against *E. coli* 8739, *E. coli* 13846, and *E. coli* 2340. The tested time is 180 min, and the treated concentrations of peptide range from 1 × MIC to 4 × MIC. Untreated cells are set as the growth control. DMSO (1 %) treated cells are set as the vehicle control group.

of 0.2, indicating a weaker binding capacity to the plasmid DNA compared to des-Ala^{16}-[Lys^{4}]brevinin-1pl (Fig. 7c). The molecular docking result reveals that the interaction between the DNA duplex and des-Ala^{16}-[Lys^{4}]brevinin-1pl is driven by hydrogen bonds and pi stacking, which are formed between the 1st and 2nd Phe residues of the peptide and sites within the DNA minor groove (Fig. 7d).

3.9. In vivo anti-drug resistant E. coli activities of brevinin-1pl-del 16

The *in vivo* antibacterial activities of des-Ala^{16}-[Lys^{4}]brevinin-1pl against drug-resistant *E. coli* were evaluated using the *G. mellonella* larvae model (Fig. 8). For *E. coli* 13846, the survival rate of infected larvae was only 30 % on the fifth day post-infection. Treatment with des-Ala^{16}-[Lys^{4}]brevinin-1pl significantly increased the survival rate to approximately 80 % to 90 %. Similarly, for *E. coli* 2340, the presence of des-Ala^{16}-[Lys^{4}]brevinin-1pl remarkably increased the survival rate of infected larvae from 50 % to 90 %.

3.10. Effects of brevinin-1pl and des-Ala^{16}-[Lys^{4}]brevinin-1pl on human cancer cells and non-cancerous cells

Brevinin-1pl and des-Ala^{16}-[Lys^{4}]brevinin-1pl were evaluated for their cytotoxic effects on both human cancerous cells and healthy cells. As shown in Fig. 9, both peptides demonstrated significant inhibitory effects on the growth of tested cancer cell lines when the concentration exceeded 10^{-5} M. The IC_{50} values of both peptides against both cancer cell lines are closely similar (Table 7). Although both peptides exhibited high selectivity between the tested cancer cell lines and healthy cells, the IC_{50} value of the analogue des-Ala^{16}-[Lys^{4}]brevinin-1pl (128.1 μM) is relatively higher than that of its template (IC_{50} = 62.71 μM).

4. Discussion

As a critical component of the host's innate immunity, AMPs play a crucial role in combating a wide range of microorganisms [3,6,16,52,53]. With the global emergence of antimicrobial resistance (AMR), AMPs have garnered significant attention as alternatives to traditional antibiotics [54,55]. The skin of amphibian from the Rana genus is a rich source of AMPs, with brevinins exhibiting potent antimicrobial, immunomodulatory, and anticancer properties, positioning them as promising therapeutic agents [16,17,56].

In this study, we identified a novel brevinin-1 peptide, brevinin-1pl, from the skin secretions of the frog *Rana pipiens*. Sequence alignments revealed that brevinin-1pl shares no more than 77 % similarity with reported brevinin-1 peptides and contains a C-terminal 'Rana Box' looped by a disulphide bridge. Although the role of the 'Rana Box' in frog-derived AMPs is often debated, it plays a crucial role in maintaining the helical structure and antimicrobial activity within the brevinin-1 family [14,24,57,58]. For instance, deleting the Rana Box from brevinin-1OS resulted in its derivative, Osa, completely losing its antimicrobial activity at tested concentrations [30]. A similar outcome was observed in brevinin-OG9 modifications, where the removal of the 'Rana Box' also

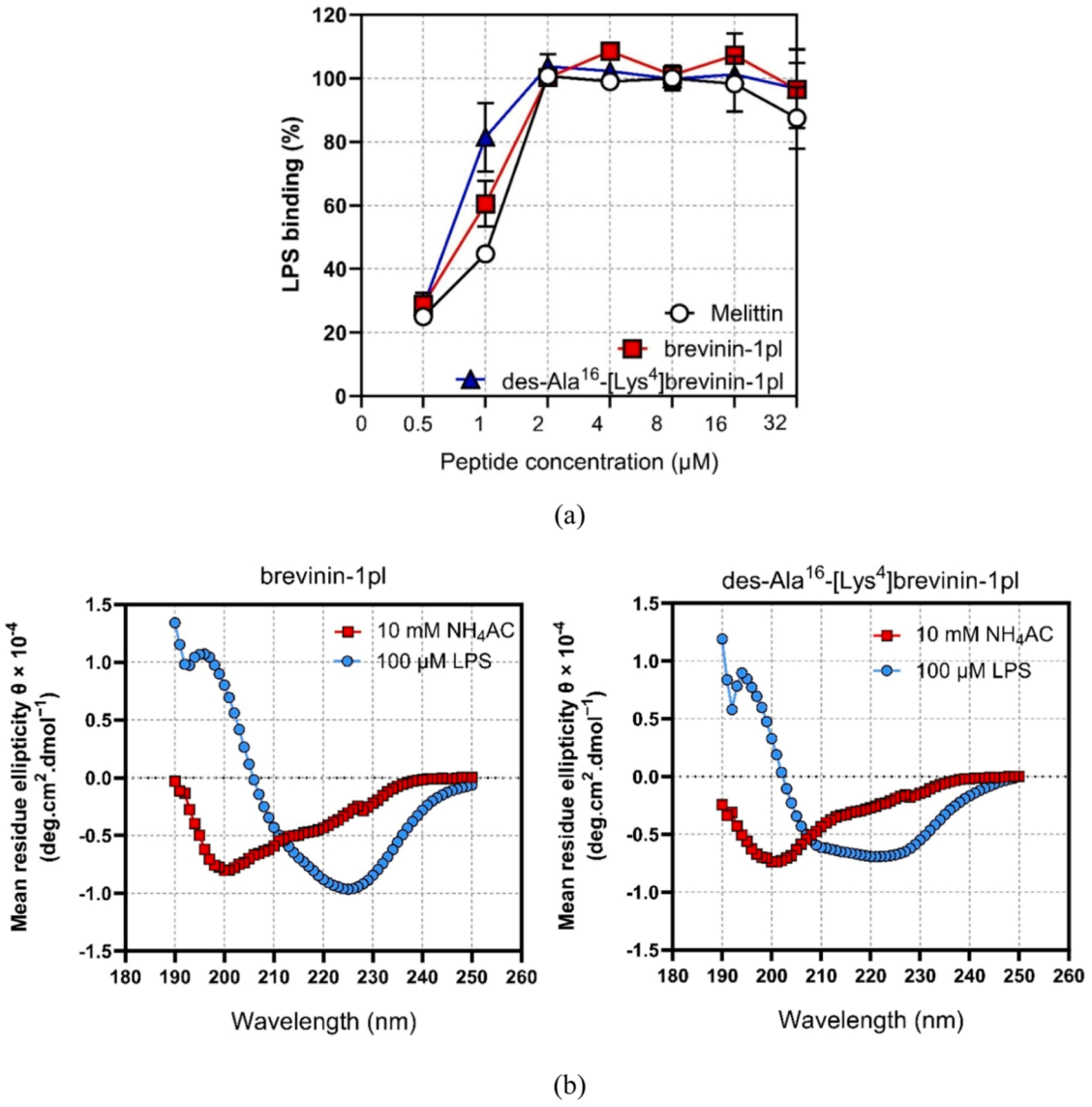

Fig. 5. (a) Binding affinity of brevinin-1pl, des-Ala^{16}-[Lys^{4}]brevinin-1pl and melittin with LPS. (b) CD spectrum of brevinin-1pl (left) and des-Ala^{16}-[Lys^{4}]brevinin-1pl (right) with or without LPS.

led to a loss of antimicrobial activity and a significant reduction in the peptide's helical content [17]. Therefore, when modifying brevinin-1pl, we chose not to alter the 'Rana Box' structure to preserve its antimicrobial activity. Instead, we focused on the N-terminal sequence, adjusting the peptide's hydrophobicity by replacing weakly hydrophobic amino acids or deleting strongly hydrophobic ones, thereby controlling the peptide's potential toxicity to some extent [59]. Like many reported brevinin-1 peptides, brevinin-1pl demonstrated potent antibacterial activity against both Gram-positive and Gram-negative bacteria [2,22–24,26]. This activity may be attributed to several structural characteristics of brevinin-1pl, including its net charge, hydrophobicity, and secondary structure. The presence of five net-positive charged residues within the brevinin-1pl sequence may facilitate the initial electrostatic attraction between the cationic peptide and the anionic bacterial membrane, enabling brevinin-1pl to effectively target bacteria. Furthermore, the hydrophobicity of brevinin-1pl, as indicated by a hydrophobicity index of 0.765 and a large hydrophobic face composed of nine residues, allows the peptide to interact with hydrophobic regions of both bacterial and mammalian cell membranes. CD spectrum analysis of brevinin-1pl indicated a predominately α-helical structure in both NH_4AC and TFE solutions. As one of the fundamental factors affecting the interaction between the AMP and the membrane [59], the formation of the helical structure in the membrane environment enables the peptide to expose its hydrophobic residues, enhancing contact with surrounding lipid molecules and contributing to its potent antibacterial activity, as well as its haemolytic and cytotoxic effects.

CD results also revealed that several of the modified peptides exhibit a high degree of helicity, around 95 %, in their secondary structures in the TFE environment, similar to their parent peptide. This high helicity is crucial for the membrane-disrupting effect of AMPs [60]. After conducting antibacterial activity screening, it was found that the activity of the modified peptide against Gram-positive bacteria was decreased. However, the activity of des-Ala^{16}-[Lys4]brevinin-1pl against Gram-negative bacteria remained basically unchanged or even improved. The reduced antibacterial activity of brevinin-1pl analogues highlights the critical role of hydrophobicity in targeting Gram-positive bacteria, consistent with previous findings that emphasize the importance of hydrophobic residues in anti-Gram-positive peptides [49]. For Gram-negative bacteria, charged residues appear to be more critical in AMPs [61]. Since the modifications slightly increase the net charge of des-Ala^{16}-[Lys^{4}]brevinin-1pl, this may explain why their anti-Gram-negative activity remained largely unchanged or even

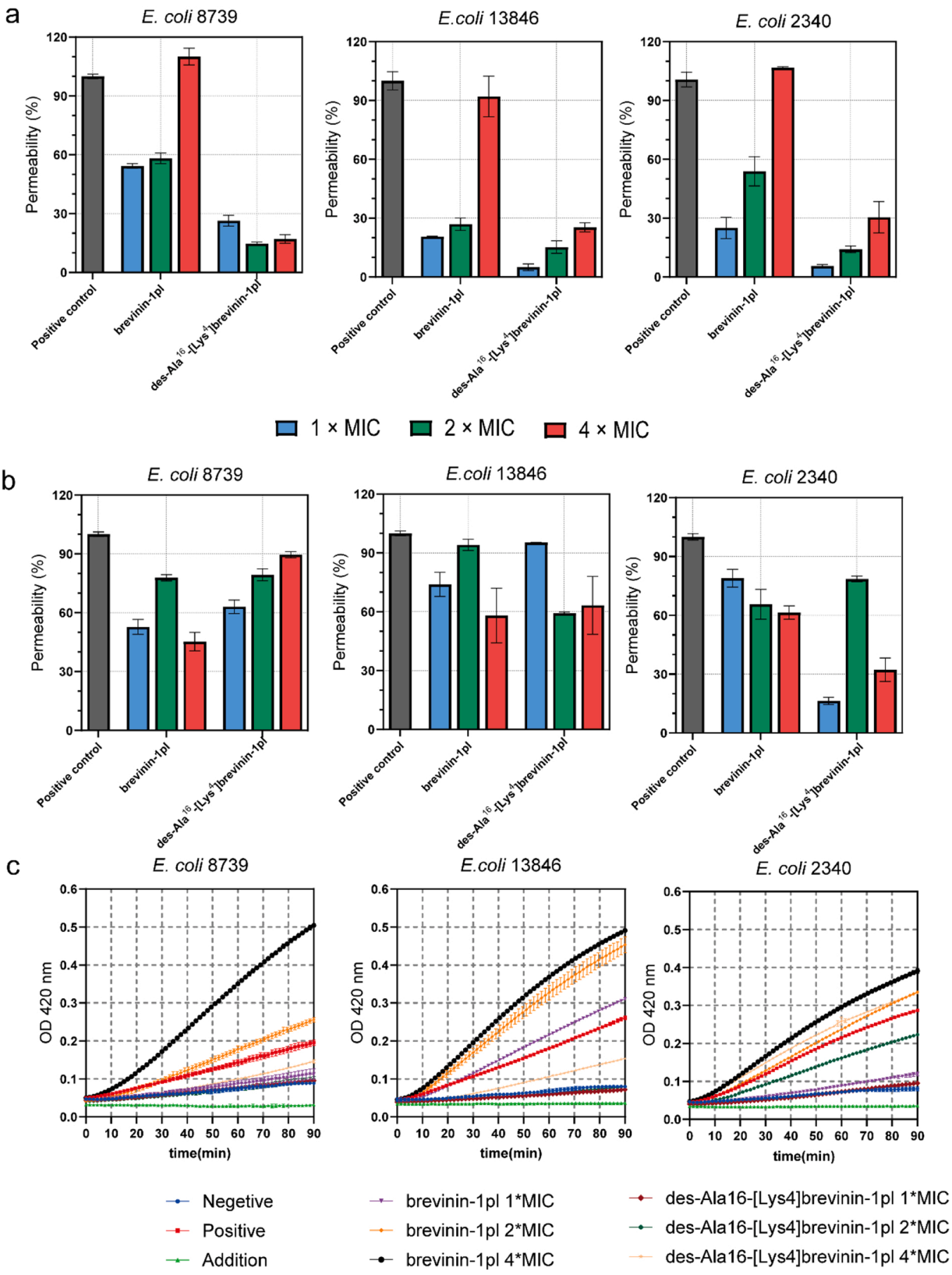

Fig. 6. Effects of brevinin-1pl and des-Ala^{16}-[Lys^{4}]brevinin-1pl on the membrane of three *E. coli* strains. (a) Changes in OM permeability in the presence or absence of peptides. The positive control is *E. coli* cells treated with melittin. (b) Changes in cytoplasmic membrane permeability in the presence or absence of peptides. Melittin is served as the positive control. (c) ONPG assay results of breinin-1pl and des-Ala^{16}-[Lys^{4}]brevinin-1pl against three *E. coli* strains. The negative group is untreated *E. coli* cells. The positive control is *E. coli* cells treated with Melittin. The addition group include only the solvent.

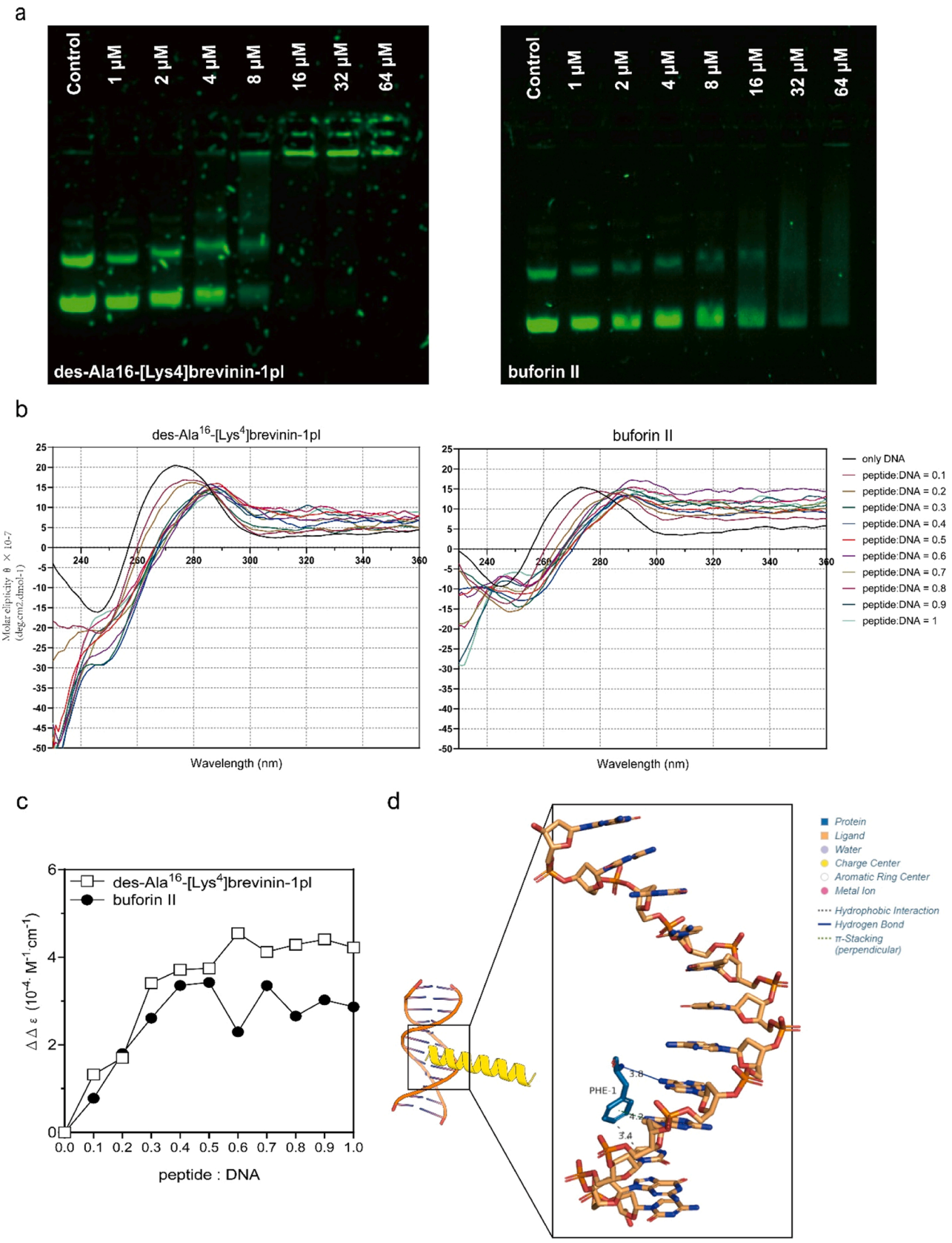

Fig. 7. Interaction of brevinin-1pl and des-Ala^{16}-[Lys^{4}]brevinin-1pl with plasmid DNA of *E. coli*. (a) Effects of des-Ala^{16}-[Lys^{4}]brevinin-1pl and buforin II on the migration of plasmid DNA (pBR322). (b) CD spectra result of des-Ala^{16}-[Lys^{4}]brevinin-1pl (left) and buforin II (right) binding with plasmid DNA. (c) The normalised changes of des-Ala^{16}-[Lys^{4}]brevinin-1pl and buforin II to the plasmid DNA in CD signal at 275 nm. (d) Molecular docking model of des-Ala^{16}-[Lys^{4}]brevinin-1pl with the DNA (PDB ID: 1BNA). The grey dash bond represents the hydrophobic interaction between the peptide and DNA. The blue bond represents formed hydrogen bonds. The green dash bond represents the π-stacking.

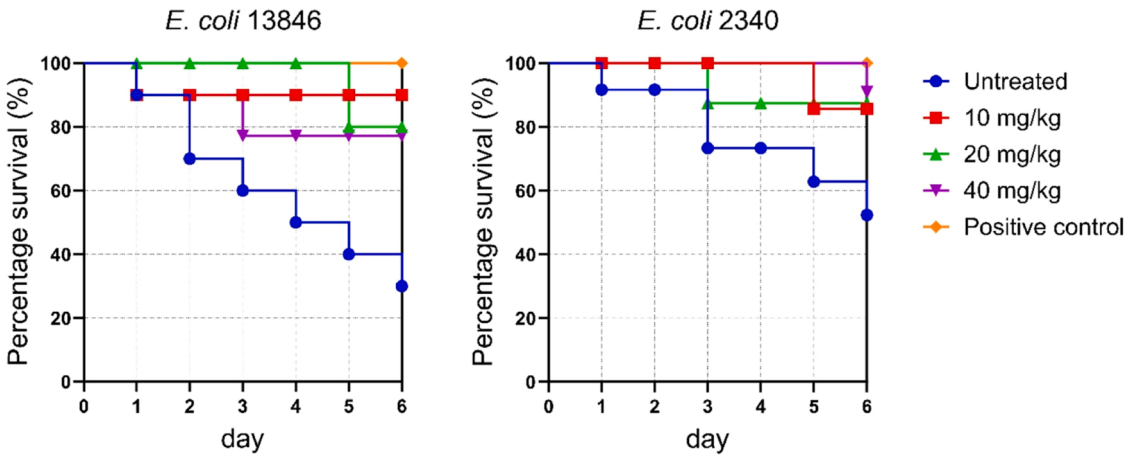

Fig. 8. The Kaplan-Meier-curves of des-Ala^{16}-[Lys^{4}]brevinin-1plin wax moth larvae infected with *E. coli* 13846 (a) and *E. coli* 2340 (b). The group of infected larvae treated with Rifampin (20 mg/kg) was set as the positive control.

improved. From the haemolytic activity screening, [Lys^{4}, Ala^{13}]brevinin-1pl and [Lys^{4}, Ala^{16}]brevinin-1pl exhibited reduced activity compared to the parent peptide, brevinin-1pl, which may be attributed to the addition of an extra positive charge. It has been demonstrated that additional positive charges can increase the haemolytic activity of AMPs [62]. The HC_{50} of [Lys^{4}, Ala$^{13, 16}$]brevinin-1pl was greater than 128 μM, indicating that the decrease in hydrophobicity could reduce the haemolytic activity. des-Ala^{16}-[Lys^{4}]brevinin-1pl and des-Leu^{13}, Ala^{16}-[Lys^{4}]brevinin-1pl both exhibited very low haemolytic activity, indicating that the reduction in hydrophobicity due to the deletion of the amino acid at the 16th position decreased the haemolytic activity of the peptides. The results of des-Ala^{16}-[Lys^{4}]brevinin-1pl further supported that reducing hydrophobicity could decrease the haemolytic activity of the peptide. Meanwhile, the experimental results of [Lys^{4}, Ala$^{13, 16}$]brevinin-1pl demonstrated that decreasing hydrophobicity and increasing amphiphilicity significantly reduced haemolytic activity. The therapeutic index calculated from the MIC concentration and HC_{10} of haemolytic activity in the results of the antimicrobial assay generally shows the degree of safety of the drug. The results of the TI values show that the modified peptide became less effective against Gram-positive bacteria, probably related to its reduced hydrophobicity. However, des-Ala^{16}-[Lys^{4}]brevinin-1pl achieved a TI index of 55.77 against Gram-negative bacteria, which is a very safe level compared to melittin's TI and that of polymyxin B (Colistin) [63,64]. In the *in vivo* antibacterial tests, des-Ala^{16}-[Lys^{4}]brevinin-1pl also exhibited potent antibacterial activities against two drug-resistant *E. coli* strains, and the survival rate of the infected group greatly improved. Modification of brevinin-1pl demonstrated that managing the hydrophobicity might be an effective strategy for controlling the toxicity of brevinin-1 peptides. Given the potential critical role of the 'Rana Box' in the bioactivity of brevinin-1 peptides, adjustments in hydrophobicity should preferably focus on the residues outside the loop. This hypothesis needs to be validated through further modifications in future studies on brevinin-1 peptides.

As the modified peptides were more effective against Gram-negative bacteria, des-Ala^{16}-[Lys^{4}]brevinin-1pl was chosen to screen for antimicrobial activity against *E. coli* NCTC 13846, which is colistin-resistant due to the mcr-1 gene, and *E. coli* BAA 2340, which contains the bla_{KPC} gene, conferring resistance to imipenem and ertapenem. The parent peptide, brevinine-1pl, was also employed as a comparison. Des-Ala^{16}-[Lys^{4}]brevinin-1pl exhibited potent antibacterial activities and higher selectivity against both drug-resistant bacteria, suggesting it may hold promise for further development as anti-infectious agents. Time-killing experiments were conducted next. The results of brevinin-1pl and des-Ala^{16}-[Lys^{4}]brevinin-1pl against three types of *E. coli* showed that all the peptides could completely clear the bacteria within 1 h at their MICs. This confirms other reports which have shown that AMPs have a fast bactericidal action [2]. To further investigate the antimicrobial mechanism, an LPS binding experiment was conducted to determine if the peptides interact with endotoxins. The results showed that brevinin-1pl and des-Ala^{16}-[Lys^{4}]brevinin-1pl had the similar ability to bind to LPS as melittin at similar concentrations. CD results demonstrated that the presence of LPS can induce conformational changes in brevinin-1pl and des-Ala^{16}-[Lys^{4}]brevinin-1pl, improving their helicity, which may facilitate their interaction with the *E. coli* membrane.

Next, a series of experiments were carried out to verify whether the peptides influenced the permeability of the *E. coli* cell membrane. First, an NPN experiment was conducted. When the outer membrane is disrupted by AMPs, NPN can enter the hydrophobic environment of the membrane and emit fluorescence. Therefore, an increase in fluorescence signal indicates that the AMP has damaged the outer membrane. The results showed that brevinin-1pl achieved a 100 % outer membrane breakage rate at four-fold MIC, while des-Ala^{16}-[Lys^{4}]brevinin-1pl had less ability to affect the permeability of the outer membrane. A SYTOX green experiment was subsequently carried out to verify the effect of the AMPs on the permeability of the cytoplasmic membrane. Generally, the permeability rate increases with increasing concentration of AMPs. However, peptides may have other mechanisms that result in membrane permeability that does not increase with concentration. To further verify the ability of AMPs to cause inner membrane damage, the ONPG experiment was performed. The results indicated that for disrupting the cell membrane, brevinin-1pl exceeded melittin at four-fold MIC. The results showed that brevinin-1pl has a strong ability to disrupt inner membrane permeability, which is stronger than melittin at four-fold MIC, indicating that brevinin-1pl may kill *E. coli* through a membrane-disruptive mechanism, similar to many reported frog AMPs.

However, the results for des-Ala^{16}-[Lys^{4}]brevinin-1pl suggest that while increased membrane permeabilisation may allow the SYTOX green dye to access the DNA, the release of beta-galactosidase still cannot pass through the membrane. This suggests that the impact of des-Ala^{16}-[Lys^{4}]brevinin-1pl on the *E. coli* membrane may be only one part of its mode of action, and other intracellular targets might exist. Therefore, we conducted several experiments to study the interaction of des-Ala^{16}-[Lys^{4}]brevinin-1pl with *E. coli* plasmid DNA. Exploration of the interaction of des-Ala^{16}-[Lys^{4}]brevinin-1pl with DNA showed that it could bind with DNA and retard its movement in gel electrophoresis. Additionally, CD results verify the presence of binding and also demonstrate that des-Ala^{16}-[Lys^{4}]brevinin-1pl exhibits a more potent DNA binding capacity than buforin II and can bend *E. coli* plasmid DNA. Mechanism studies on des-Ala^{16}-[Lys^{4}]brevinin-1pl suggest that it may exert its anti-*E. coli* functions *via* a combined mode of action, involving

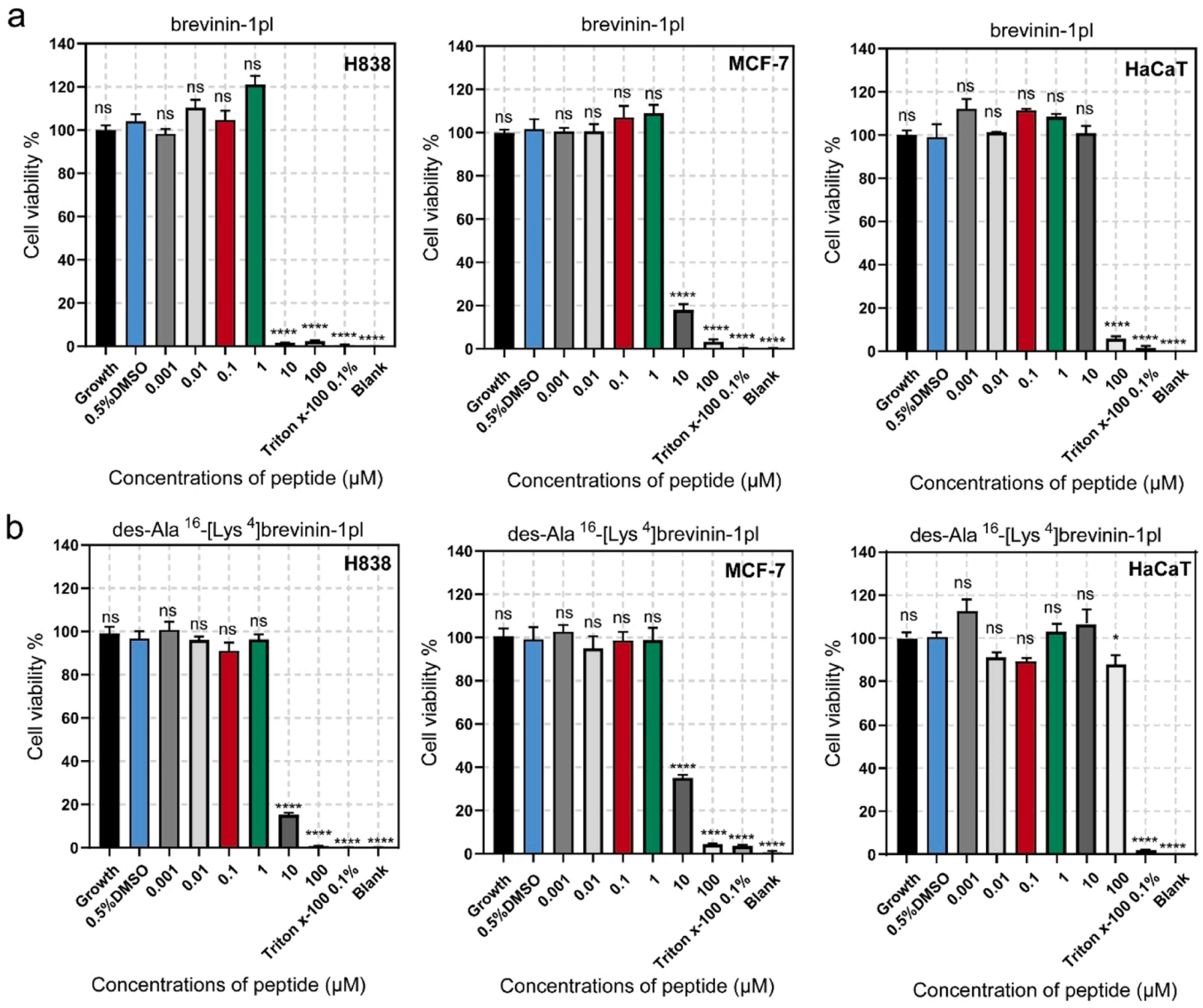

Fig. 9. Effects of brevinin-1pl (a) and des-Ala^{16}-[Lys^{4}]brevinin-1pl (b) on the growth of tested cancerous cells H838 and MCF-7 and human healthy cells HaCaT. The concentrations of tested peptides range from 10^{-9} to 10^{-4} M. Cells without treatment employed as the growth control (shown as growth in the graph). DMSO (0.5 %) was set as the vehicle control, and Triton x-100 was employed as the positive control. Growth medium was employed as the blank control. The data represented show the S.E.M. calculated from nine replicates conducted in three independent experiments. No significance (ns), * ($p < 0.05$), and * ** * ($p < 0.0001$) compared to the vehicle control group, determined by One-Way ANOVA.

Table 7
IC_{50} (μM) values of brevinin-1pl and des-Ala^{16}-[Lys^{4}]brevinin-1pl.

Peptide	H838	MCF-7	HaCaT
brevinin−1pl	6.88	7.60	62.71
des-Ala^{16}-[Lys^{4}]brevinin−1pl	4.536	7.194	128.1

both membrane disruption and DNA/RNA binding. This combined mode of action may also reduce the likelihood of the peptide inducing drug resistance compared to peptides or antibiotics that target a single mechanism. In the *in vivo* antibacterial tests, des-Ala^{16}-[Lys^{4}]brevinin-1pl exhibited potent antibacterial activity against two drug-resistant *E. coli* strains, remarkably improving the survival rate of the infected group, further demonstrating its great potential to be developed into a novel antimicrobial drug.

MTT assays were conducted to test the peptide cytotoxicity. Both electrostatic contact and hydrophobic effects contribute to the selectivity of the AMPs against bacteria and cancer cells [65]. The experimental results showed that both brevinine-1pl and des-Ala^{16}-[Lys^{4}]brevinin-1pl exhibited significant inhibitory effects on both H838 and MCF-7 cancer cell lines, while the selectivity of des-Ala^{16}-[Lys^{4}]brevinin-1pl was higher than that of the parent peptide brevinine-1pl. Considering the anti-*E. coli* activities and haemolysis together, the analogue des-Ala^{16}-[Lys^{4}]brevinin-1pl may effectively exert its antibacterial functions without inducing significant toxicity to the body and holds great promise for further development.

5. Conclusion

In this study, we identified a novel brevinin-1 peptide, brevinin-1pl, from the skin secretion of the frog, *Rana pipiens*, and employed a set of bioinformatics tools to design several analogues aimed at improving the therapeutic potential of brevinin-1 peptides. The optimal analogue, des-Ala^{16}-[Lys^{4}]brevinin-1pl, with high therapeutic efficacy, was successfully developed. It displayed potent antibacterial activity against drug-resistant *E. coli* in both *in vitro* and *in vivo* tests, and it kills bacteria *via* a combined mode of action, including membrane disruption and DNA/

RNA targeting. In summary, the modifications on brevinin-1pl provide valuable insights for improving brevinin-1 peptides in future research, and the analogue des-Ala^{16}-[Lys^{4}]brevinin-1pl may be a promising candidate for further development as an antibacterial agent.

Funding

This research received no external funding.

CRediT authorship contribution statement

Tianbao Chen: Supervision, Conceptualization. **Chris Shaw:** Writing – review & editing. **Yangyang Jiang:** Writing – review & editing, Supervision, Methodology. **Tao Wang:** Writing – review & editing, Methodology. **Xiaoling Chen:** Visualization, Methodology. **Chengbang Ma:** Project administration. **Jibo Hu:** Software, Methodology, Investigation, Data curation. **Wenyuan Pu:** Visualization, Software, Methodology. **Lei Wang:** Writing – review & editing, Supervision, Methodology. **Jingkai Wang:** Writing – original draft, Investigation, Formal analysis. **Mei Zhou:** Supervision, Resources, Conceptualization.

Declaration of Competing Interest

The authors declare that they have no known competing financial interests or personal relationships that could have appeared to influence the work reported in this paper.

Appendix A. Supporting information

Supplementary data associated with this article can be found in the online version at doi:10.1016/j.csbj.2024.09.006.

References

[1] Murray CJ, Ikuta KS, Sharara F, Swetschinski L, Robles Aguilar G, Gray A, et al. Global burden of bacterial antimicrobial resistance in 2019: a systematic analysis. Lancet 2022;399. https://doi.org/10.1016/S0140-6736(21)02724-0.
[2] Zou W, Sun R, Yao A, Zhou M, Chen X, Ma C, et al. A promising antibiotic candidate, brevinin-1 analogue 5R, against drug-resistant bacteria, with insights into its membrane-targeting mechanism. Comput Struct Biotechnol J 2023;21: 5719–37. https://doi.org/10.1016/j.csbj.2023.11.031.
[3] Zhang QY, Yan ZBin, Meng YM, Hong XY, Shao G, Ma JJ, et al. Antimicrobial peptides: mechanism of action, activity and clinical potential. Mil Med Res 2021;8. https://doi.org/10.1186/s40779-021-00343-2.
[4] Prestinaci F, Pezzotti P, Pantosti A. Antimicrobial resistance: a global multifaceted phenomenon. Pathog Glob Health 2015;109. https://doi.org/10.1179/2047773215Y.0000000030.
[5] Mahlapuu M, Björn C, Ekblom J. Antimicrobial peptides as therapeutic agents: opportunities and challenges. Crit Rev Biotechnol 2020;40. https://doi.org/10.1080/07388551.2020.1796576.
[6] Wang J, Dou X, Song J, Lyu Y, Zhu X, Xu L, et al. Antimicrobial peptides: promising alternatives in the post feeding antibiotic era. Med Res Rev 2019;39. https://doi.org/10.1002/med.21542.
[7] Shi J, Chen C, Wang D, Wang Z, Liu Y. The antimicrobial peptide LI14 combats multidrug-resistant bacterial infections. Commun Biol 2022;5. https://doi.org/10.1038/s42003-022-03899-4.
[8] Talapko J, Meštrović T, Juzbašić M, Tomas M, Erić S, Horvat Aleksijević L, et al. Antimicrobial peptides—mechanisms of action, antimicrobial effects and clinical applications. Antibiotics 2022;11. https://doi.org/10.3390/antibiotics11101417.
[9] Bhattacharjya S, Straus SK. Design, engineering and discovery of novel α-helical and β-boomerang antimicrobial peptides against drug resistant bacteria. Int J Mol Sci 2020;21. https://doi.org/10.3390/ijms21165773.
[10] Kumar A, Mahajan M, Awasthi B, Tandon A, Harioudh MK, Shree S, et al. Piscidin-1-analogs with double L- and D-lysine residues exhibited different conformations in lipopolysaccharide but comparable anti-endotoxin activities. Sci Rep 2017;7. https://doi.org/10.1038/srep39925.
[11] Casciaro B, Cappiello F, Loffredo MR, Ghirga F, Mangoni ML. The potential of frog skin peptides for anti-infective therapies: the case of Esculentin-1a(1-21)NH2. Curr Med Chem 2019;27. https://doi.org/10.2174/0929867326666190722095408.
[12] Ma R, Kwok HF. New opportunities and challenges of venom-based and bacteria-derived molecules for anticancer targeted therapy. Semin Cancer Biol 2022;80. https://doi.org/10.1016/j.semcancer.2020.08.010.
[13] Ma R, Wong SW, Ge L, Shaw C, Siu SWI, Kwok HF. In vitro and MD simulation study to explore physicochemical parameters for antibacterial peptide to become potent anticancer peptide. Mol Ther Oncolytics 2020;16. https://doi.org/10.1016/j.omto.2019.12.001.
[14] Liu X, Shi D, Cheng S, Chen X, Ma C, Jiang Y, et al. Modification and synergistic studies of a novel frog antimicrobial peptide against Pseudomonas aeruginosa biofilms. Antibiotics 2024;13. https://doi.org/10.3390/antibiotics13070574.
[15] Mookherjee N, Anderson MA, Haagsman HP, Davidson DJ. Antimicrobial host defence peptides: functions and clinical potential. Nat Rev Drug Discov 2020;19. https://doi.org/10.1038/s41573-019-0058-8.
[16] Kumari T, Verma DP, Afshan T, Verma NK, Pant G, Ali M, et al. A noncytotoxic Temporin L analogue with in vivo antibacterial and antiendotoxin activities and a nonmembrane-lytic mode of action. ACS Infect Dis 2020;6. https://doi.org/10.1021/acsinfecdis.0c00022.
[17] Fei F, Wang T, Jiang Y, Chen X, Ma C, Zhou M, et al. A frog-derived antimicrobial peptide as a potential anti-biofilm agent in combating Staphylococcus aureus skin infection. J Cell Mol Med 2023;27. https://doi.org/10.1111/jcmm.17785.
[18] Xu X, Lai R. The chemistry and biological activities of peptides from amphibian skin secretions. Chem Rev 2015;115. https://doi.org/10.1021/cr4006704.
[19] König E, Bininda-Emonds ORP, Shaw C. The diversity and evolution of anuran skin peptides. Pept (N Y) 2015;63. https://doi.org/10.1016/j.peptides.2014.11.003.
[20] Ladram A, Nicolas P. Antimicrobial peptides from frog skin: biodiversity and therapeutic promises. Front Biosci - Landmark 2016;21. https://doi.org/10.2741/4461.
[21] Savelyeva A, Ghavami S, Davoodpour P, Asoodeh A, Łos MJ. An overview of brevinin superfamily: Structure, function and clinical perspectives. Adv Exp Med Biol 2014;818. https://doi.org/10.1007/978-1-4471-6458-6_10.
[22] Tian M, Wang K, Liang Y, Chai J, Wu J, Zhang H, et al. The first Brevinin-1 antimicrobial peptide with LPS-neutralizing and anti-inflammatory activities in vitro and in vivo. Front Microbiol 2023;14. https://doi.org/10.3389/fmicb.2023.1102576.
[23] Ju X, Fan D, Kong L, Yang Q, Zhu Y, Zhang S, et al. Antimicrobial peptide Brevinin-1RL1 from frog skin secretion induces apoptosis and necrosis of tumor cells. Molecules 2021;26. https://doi.org/10.3390/molecules26072059.
[24] Jiang Y, Wu Y, Wang T, Chen X, Zhou M, Ma C, et al. Brevinin-1GHD: a novel Hylarana guentheri skin secretion-derived Brevinin-1 type peptide with antimicrobial and anticancer therapeutic potential. Biosci Rep 2020;40. https://doi.org/10.1042/BSR20200019.
[25] Qin H, Zuo W, Ge L, Siu SWI, Wang L, Chen X, et al. Discovery and analysis of a novel antimicrobial peptide B1AW from the skin secretion of Amolops wuyiensis and improving the membrane-binding affinity through the construction of the lysine-introduced analogue. Comput Struct Biotechnol J 2023;21. https://doi.org/10.1016/j.csbj.2023.05.006.
[26] Pál T, Abraham B, Sonnevend Á, Jumaa P, Conlon JM. Brevinin-1BYa: a naturally occurring peptide from frog skin with broad-spectrum antibacterial and antifungal properties. Int J Antimicrob Agents 2006;27. https://doi.org/10.1016/j.ijantimicag.2006.01.010.
[27] Li W, Separovic F, O'Brien-Simpson NM, Wade JD. Chemically modified and conjugated antimicrobial peptides against superbugs. Chem Soc Rev 2021;50. https://doi.org/10.1039/d0cs01026j.
[28] Domadia PN, Bhunia A, Ramamoorthy A, Bhattacharjya S. Structure, interactions, and antibacterial activities of MSI-594 derived mutant peptide MSI-594F5A in lipopolysaccharide micelles: role of the helical hairpin conformation in outer-membrane permeabilization. J Am Chem Soc 2010;132. https://doi.org/10.1021/ja1083255.
[29] Saravanan R, Bhunia A, Bhattacharjya S. Micelle-bound structures and dynamics of the hinge deleted analog of melittin and its diastereomer: Implications in cell selective lysis by d-amino acid containing antimicrobial peptides. Biochim Biophys Acta Biomembr 2010;1798. https://doi.org/10.1016/j.bbamem.2009.07.014.
[30] Zhou X, Liu Y, Gao Y, Wang Y, Xia Q, Zhong R, et al. Enhanced antimicrobial activity of N-terminal derivatives of a novel Brevinin-1 peptide from the skin secretion of Odorrana schmackeri. Toxins 2020;12. https://doi.org/10.3390/toxins12080484.
[31] Chen T, Zhou M, Rao P, Walker B, Shaw C. The Chinese bamboo leaf odorous frog (Rana (Odorrana) versabilis) and North American Rana frogs share the same families of skin antimicrobial peptides. Peptides 2006;27. https://doi.org/10.1016/j.peptides.2006.02.009.
[32] Zhou X, Shi D, Zhong R, Ye Z, Ma C, Zhou M, et al. Bioevaluation of ranatuerin-2Pb from the frog skin secretion of Rana pipiens and its truncated analogues. Biomolecules 2019;9. https://doi.org/10.3390/biom9060249.
[33] Lamiable A, Thevenet P, Rey J, Vavrusa M, Derreumaux P, Tuffery P. PEP-FOLD3: faster denovo structure prediction for linear peptides in solution and in complex. Nucleic Acids Res 2016;44. https://doi.org/10.1093/nar/gkw329.
[34] Gautier R, Douguet D, Antonny B, Drin G. HELIQUEST: A web server to screen sequences with specific α-helical properties. Bioinformatics 2008;24. https://doi.org/10.1093/bioinformatics/btn392.
[35] Lomize AL, Todd SC, Pogozheva ID. Spatial arrangement of proteins in planar and curved membranes by PPM 3.0. Protein Sci 2022;31. https://doi.org/10.1002/pro.4219.
[36] Yan Y, Tao H, He J, Huang SY. The HDOCK server for integrated protein–protein docking. Nat Protoc 2020;15. https://doi.org/10.1038/s41596-020-0312-x.
[37] Adasme MF, Linnemann KL, Bolz SN, Kaiser F, Salentin S, Haupt VJ, et al. PLIP 2021: expanding the scope of the protein-ligand interaction profiler to DNA and RNA. Nucleic Acids Res 2021;49. https://doi.org/10.1093/nar/gkab294.
[38] Tam JP, Wu CR, Liu W, Zhang JW. Disulfide bond formation in peptides by dimethyl sulfoxide. scope and applications. J Am Chem Soc 1991;113. https://doi.org/10.1021/ja00017a044.
[39] Cary PD, Kneale GG. Circular dichroism for the analysis of protein-DNA interactions. Methods Mol Biol 2009;543. https://doi.org/10.1007/978-1-60327-015-1_36.

[40] Carpenter ML, Oliver AW, Kneale GG. Circular dichroism for the analysis of protein-DNA interactions. Methods Mol Biol 2001;148. https://doi.org/10.1385/1-59259-208-2:503.
[41] Louis-Jeune C, Andrade-Navarro MA, Perez-Iratxeta C. Prediction of protein secondary structure from circular dichroism using theoretically derived spectra. Protein Struct, Funct Bioinform 2012;80. https://doi.org/10.1002/prot.23188.
[42] Zou W, Zhang Y, Zhou M, Chen X, Ma C, Wang T, et al. Exploring the active core of a novel antimicrobial peptide, palustrin-2LTb, from the Kuatun frog, Hylarana latouchii, using a bioinformatics-directed approach. Comput Struct Biotechnol J 2022;20:6192–205. https://doi.org/10.1016/j.csbj.2022.11.016.
[43] Zai Y, Xi X, Ye Z, Ma C, Zhou M, Chen X, et al. Aggregation and its influence on the bioactivities of a novel antimicrobial peptide, temporin-pf, and its analogues. Int J Mol Sci 2021;22. https://doi.org/10.3390/ijms22094509.
[44] Chen G, Miao Y, Ma C, Zhou M, Shi Z, Chen X, et al. Brevinin-2GHK from sylvirana guentheri and the design of truncated analogs exhibiting the enhancement of antimicrobial activity. Antibiotics 2020;9. https://doi.org/10.3390/antibiotics9020085.
[45] Li L, Wu Q, Wang X, Lu H, Xi X, Zhou M, et al. Discovery of novel caeridins from the skin secretion of the Australian White's Tree Frog, Litoria caerulea. Int J Genom 2018;2018. https://doi.org/10.1155/2018/8158453.
[46] Ma X, Chen Y, Shu A, Jiang Y, Chen X, Ma C, et al. A novel antimicrobial peptide, Dermaseptin-SS1, with anti-proliferative activity, isolated from the skin secretion of Phyllomedusa tarsius. Molecules 2023;28. https://doi.org/10.3390/molecules28186558.
[47] Nam J, Yun H, Rajasekaran G, Kumar SD, Kim JIl, Min HJ, et al. Structural and functional assessment of mBjAMP1, an antimicrobial peptide from Branchiostoma japonicum, revealed a novel α-hairpinin-like scaffold with membrane permeable and DNA binding activity. J Med Chem 2018;61. https://doi.org/10.1021/acs.jmedchem.8b01135.
[48] Lai Z, Tan P, Zhu Y, Shao C, Shan A, Li L. Highly stabilized α-Helical coiled coils kill gram-negative bacteria by multicomplementary mechanisms under acidic condition. ACS Appl Mater Interfaces 2019;11:22113–28. https://doi.org/10.1021/acsami.9b04654.
[49] Wang Z, Ding W, Shi D, Chen X, Ma C, Jiang Y, et al. Functional characterisation and modification of a novel Kunitzin peptide for use as an anti-trypsin antimicrobial peptide against drug-resistant Escherichia coli. Biochem Pharm 2024;229:116508. https://doi.org/10.1016/j.bcp.2024.116508.
[50] Park CB, Kim HS, Kim SC. Mechanism of action of the antimicrobial peptide buforin II: Buforin II kills microorganisms by penetrating the cell membrane and inhibiting cellular functions. Biochem Biophys Res Commun 1998;244. https://doi.org/10.1006/bbrc.1998.8159.
[51] Yao A, Liu T, Cai Y, Zhou S, Chen X, Zhou M, et al. Progressive design of a Ranatuerin-2 peptide from Amolops wuyiensis: enhancement of bioactivity and in vivo efficacy. Antibiotics 2024;13. https://doi.org/10.3390/antibiotics13010005.
[52] Duarte-Mata DI, Salinas-Carmona MC. Antimicrobial peptides´immune modulation role in intracellular bacterial infection. Front Immunol 2023;14. https://doi.org/10.3389/fimmu.2023.1119574.
[53] Wang G. Human antimicrobial peptides and proteins. Pharmaceuticals 2014;7. https://doi.org/10.3390/ph7050545.
[54] Elbediwi M, Rolff J. Metabolic pathways and antimicrobial peptide resistance in bacteria. J Antimicrob Chemother 2024:dkae128. https://doi.org/10.1093/jac/dkae128.
[55] Geitani R, Moubareck CA, Xu Z, Karam Sarkis D, Touqui L. Expression and roles of antimicrobial peptides in innate defense of airway mucosa: potential implication in cystic fibrosis. Front Immunol 2020;11. https://doi.org/10.3389/fimmu.2020.01198.
[56] Zohrab F, Askarian S, Jalili A, Kazemi Oskuee R. Biological properties, current applications and potential therapeautic applications of brevinin peptide superfamily. Int J Pept Res Ther 2019;25. https://doi.org/10.1007/s10989-018-9723-8.
[57] Lu C, Liu L, Ma C, Di L, Chen T. A novel antimicrobial peptide found in Pelophylax nigromaculatus. J Genet Eng Biotechnol 2022;20. https://doi.org/10.1186/s43141-022-00366-9.
[58] Bao K, Yuan W, Ma C, Yu X, Wang L, Hong M, et al. Modification targeting the "Rana Box" motif of a novel nigrocin peptide from Hylarana latouchii enhances and broadens its potency against multiple bacteria. Front Microbiol 2018;9. https://doi.org/10.3389/fmicb.2018.02846.
[59] Tan P, Fu H, Ma X. Design, optimization, and nanotechnology of antimicrobial peptides: from exploration to applications. Nano Today 2021;39. https://doi.org/10.1016/j.nantod.2021.101229.
[60] Huang Y, Huang J, Chen Y. Alpha-helical cationic antimicrobial peptides: relationships of structure and function. Protein Cell 2010;1. https://doi.org/10.1007/s13238-010-0004-3.
[61] Wu W, Song J, Li T, Li W, Wang J, Wang S, et al. Unlocking antibacterial potential: key-site-based regulation of antibacterial spectrum of peptides. J Med Chem 2024;67. https://doi.org/10.1021/acs.jmedchem.3c02404.
[62] Jiang Z, Vasil AI, Hale JD, Hancock REW, Vasil ML, Hodges RS. Effects of net charge and the number of positively charged residues on the biological activity of amphipathic α-helical cationic antimicrobial peptides. Biopolym Pept Sci Sect 2008;90. https://doi.org/10.1002/bip.20911.
[63] Ahn M, Gunasekaran P, Rajasekaran G, Kim EY, Lee SJ, Bang G, et al. Pyrazole derived ultra-short antimicrobial peptidomimetics with potent anti-biofilm activity. Eur J Med Chem 2017;125. https://doi.org/10.1016/j.ejmech.2016.09.071.
[64] Tsuji BT, Pogue JM, Zavascki AP, Paul M, Daikos GL, Forrest A, et al. International consensus guidelines for the optimal use of the polymyxins: endorsed by the American College of Clinical Pharmacy (ACCP), European Society of Clinical Microbiology and Infectious Diseases (ESCMID), Infectious Diseases Society of America (IDSA), International Society for Anti-infective Pharmacology (ISAP), Society of Critical Care Medicine (SCCM), and Society of Infectious Diseases Pharmacists (SIDP). Pharmacotherapy 2019;39. https://doi.org/10.1002/phar.2209.
[65] Xuan J, Feng W, Wang J, Wang R, Zhang B, Bo L, et al. Antimicrobial peptides for combating drug-resistant bacterial infections. Drug Resist Updates 2023;68. https://doi.org/10.1016/j.drup.2023.100954.